Distinct response to dioxin in an arylhydrocarbon receptor (AHR)-humanized mouse

Takashi Moriguchi*, Hozumi Motohashi*†, Tomonori Hosoya*‡, Osamu Nakajima*, Satoru Takahashi*, Seiichiroh Ohsako†§, Yasunobu Aoki†§, Noriko Nishimura†§, Chiharu Tohyama†§, Yoshiaki Fujii-Kuriyama*†‡, and Masayuki Yamamoto*†‡¶

*Institute of Basic Medical Sciences, Center for Tsukuba Advanced Research Alliance, and ‡Exploratory Research for Advanced Technology Environmental Response Project, University of Tsukuba, Tsukuba 305-8575, Japan; §Environmental Health Sciences Division, National Institute for Environmental Studies, Onogawa, Tsukuba 305-8506 Japan; and †Core Research for Evolutional Science and Technology, Japan Science and Technology Corporation, Kawaguchi 332-0012, Japan

There are large inter- and intraspecies differences in susceptibility to dioxin-induced toxicities. A critical question in risk assessment of dioxin and related compounds is whether humans are sensitive or resistant to their toxicities. The diverse responses of mammals to dioxin are strongly influenced by functional polymorphisms of the arylhydrocarbon receptor (AHR). To characterize responses mediated by the human AHR (hAHR), we generated a mouse possessing hAHR instead of mouse AHR. Responses of these mice to 2,3,7,8-tetrachlorodibenzo-p-dioxin (TCDD) and 3-methylcholanthrene were compared with the responses of naturally sensitive (C57BL/6J) and resistant (DBA/2) mice. Mice homozygous for hAHR exhibited weaker induction of AHR target genes such as $cyp1a1$ and $cyp1a2$ than did C57BL/6J ($Ahr^{b-1/b-1}$) mice. DBA/2 ($Ahr^{d/d}$) mice were less responsive to induction of cyp genes than C57BL/6J mice. hAHR and DBA/2 AHR exhibit similar ligand-binding affinities and homozygous hAHR and $Ahr^{d/d}$ mice displayed comparable induction of AHR target genes by 3-methylcholanthrene. However, when TCDD was administered, a greatly diminished response was observed in homozygous hAHR mice compared with $Ahr^{d/d}$ mice, indicating that hAHR expressed in mice is functionally less responsive to TCDD than DBA/2 AHR. After maternal exposure to TCDD, homozygous hAHR fetuses developed embryonic hydronephrosis, but not cleft palate, whereas fetuses possessing Ahr^{b-1} or Ahr^d developed both anomalies. These results suggest that hAHR may define the specificity of the responses to various AHR ligands. Thus, the hAHR knock-in mouse is a humanized model mouse that may better predict the biological effects of bioaccumulative environmental toxicants like TCDD in humans.

human | C57BL6/J | DBA/2 | CYP1A1

Polycyclic aromatic hydrocarbons (PAH) and halogenated aromatic hydrocarbons (HAH), including 2,3,7,8-tetrachlorodibenzo-p-dioxin (TCDD), benzo[a]pyrene, and polychlorinated biphenyls, are ubiquitous environmental toxicants whose chemical stability and lipophilicity make them highly persistent in the environment and in living organisms. These groups of chemicals cause various toxicological and biological responses, typified by teratogenesis, thymic atrophy, severe epithelial disorders, wasting syndrome, tumor promotion, and induction of xenobiotic-metabolizing enzymes in experimental animals (1, 2). The toxicities of these compounds are mediated by a conserved signaling pathway (1–4) through binding to and activation of the arylhydrocarbon receptor (AHR). AHR activation in turn mediates a transcriptional response for genes regulated by this transcription factor (5–8). Despite strong conservation of this pathway, there are wide inter- and intraspecies differences in the toxicological responses to AHR ligands (9–11). The molecular basis for these species and strain differences appears to relate to polymorphisms in AHR. Factors influencing susceptibility to the toxicity of TCDD have been studied in several animal models. There is a 10-fold difference in susceptibility between the dioxin-sensitive C57BL/6 and the resistant DBA/2 strains of mice that can be explained by polymorphic variations in the ligand-binding domain and in the C-terminal region of the AHR molecule of each strain (9, 12–14). Response to TCDD in the Long–Evans (sensitive) and Han/Wistar rats (resistant) differs by >1,000-fold due to a critical point mutation in the transactivation domain in the AHR of the Han/Wistar rat (15–17).

The effects of TCDD on humans are less well understood, although high incidences of chloracne, teratogenicity, and abortion have been associated with high blood concentrations of dioxin and related compounds in residents of regions where industrial accidents or extensive use of dioxin-containing defoliants have resulted in human exposures (3). Increased levels of dioxin in the body have been reported recently to be associated with abnormal sex ratio of newborns nearly 25 years after the accident in Seveso, Italy (18). Because the AHR primarily mediates the pleiotropic manifestations of dioxin exposure, characterization of the structural and functional properties of the human AHR (hAHR) is critical for understanding the types and magnitudes of human responses to various PAH/HAHs.

To date, *in vitro* characterization of the hAHR has provided ambiguous insights into human sensitivity to dioxin. The dissociation constant (K_d) of hAHR for TCDD was comparable to that of TCDD-resistant DBA/2 AHR (9, 19), suggesting that humans might be resistant to TCDD. By contrast, high homology of the human receptor to the AHR of the guinea pig, which is the most sensitive animal to TCDD, suggests a high responsiveness of humans to the toxin (20). Ligand specificity of hAHR was also examined and compared with those of zebrafish and rainbow trout AHRs using polychlorinated dibenzo-p-dioxin, dibenzofuran, and biphenyl congeners as test ligands. These studies revealed that mono-ortho polychlorinated biphenyls activated hAHR but were not very effective in activating either zebrafish or rainbow trout AHRs (21).

Assessment of human responses *in vivo* to unintended exposures to various PAH/HAHs has been hampered by limited exposure assessments and toxicological follow-up. Observational studies after intentional exposures have not been and should not be conducted. To gain stronger insight into the hazards to human health posed by compounds interacting with the hAHR *in vivo*, we generated a mouse model that harbors the hAHR cDNA instead of the mouse *AhR* gene. This mouse may reveal a humanized susceptibility to chemical toxicities. In response to challenges with 3-methylcholanthrene (3-MC) and TCDD, two prototypical AHR ligands, the hAHR knock-in

mouse displayed a distinct response profile compared with control animals harboring either the C57BL/6 *Ahr* allele (*Ahr*[b-1]) (TCDD-sensitive C57BL/6J AHR) or the DBA/2 *Ahr* allele (*Ahr*[d]) (TCDD-resistant DBA/2 AHR) in the same C57BL/6J genetic background. Although gene expression responses mediated by hAHR from 3-MC were comparable to that by DBA/2 AHR, the homozygous human AHR knock-in allele (h*AHR*) mouse was the weakest responder to TCDD among the three strains examined. These results suggest that hAHR molecules expressed in mice retain a functional human specificity that can be distinguished from the murine AHR and provide important insights into the toxicological susceptibility of humans to AHR ligands released into the environment.

Materials and Methods

Construction of the hAHR Knock-in Vector. The hAHR knock-in vector was constructed by using 129SV/J mouse *Ahr* genomic clones and hAHR cDNA as described (22). A 2-kb *Bam*HI/*Hph*I fragment containing the 129SV/J *Ahr* promoter was ligated to the hAHR cDNA (9, 22). The *neo* gene cassette was fused to the 3' end of the hAHR cDNA in a reverse orientation, followed by a 6.5-kb *Hind*III/*Eco*RI fragment of the 129SV/J *Ahr* gene. This construct was ligated to the thymidine kinase cassette on the 5' end.

Generation of hAHR Knock-in Mice. The knock-in vector was electroporated into E14 embryonic stem (ES) cells (23). A pair of primers (sense, GTATGCATTACCATGCTCCCATTCT-GCTGG; antisense, ACATCTTGTGGGAAAGGCAGCAG-GCTAGCC) was used for PCR screening. After confirmation by Southern blot analysis, positive clones were injected into blastocysts. Heterozygous hAHR knock-in mice were backcrossed into a C57BL/6J background up to the seventh generation and interbred to yield heterozygous and homozygous h*AHR* and wild-type *Ahr*[b-1/b-1] mice. The genotype of each pup was determined by PCR, with a common sense primer; 5'-ATGAG-CAGCGGCGCCAACAT-3', an antisense primer for endogenous *Ahr* allele; 5'-GCTAGACGGCACTAGGTAGG-3', and an antisense primer for targeted allele; 5'-CAGGTAACT-GACGCTGAGCC-3'. PCR amplification was carried out for 30 cycles under the following conditions; 94°C for 30 sec, 62°C for 30 sec, and 72°C for 30 sec.

Chemicals and Animals. TCDD (99.5% pure) and 3-MC were purchased from Cambridge Isotope Laboratories (Andover, MA) and Wako Pure Chemical (Osaka), respectively. D2N-*Ahrd* mice and inbred C57BL6/J mice were procured from The Jackson Laboratory. *Ahr*-null mutant mice used in this study were generated by Y.F.-K (22).

RNA Blotting Analyses. We isolated total RNA by using ISOGEN (Nippon Gene, Tokyo) and purified polyA RNA by using an Oligotex-MAG mRNA purification kit (Takara Biotechnology, Tokyo). For detection of Ahr mRNA, 5 μg of polyA RNA per lane was applied, and a portion of mouse Ahr[b-1] cDNA (*Bpu*11021-*Kpn*I; 734-bp) encoding the PAS domain was used for a probe. This nucleotide sequence is conserved with 83% homology to the corresponding hAHR cDNA (12, 24). To examine the inducibility of *CYP1A1* and *CYP1A2*, 6-week-old littermates (*Ahr*[b-1/b-1] and homozygous h*AHR*) and D2N-*Ahrd* (*Ahr*[d/d]) mice were given a single i.p. injection of 80 mg/kg 3-MC or 100 μg/kg TCDD. Mice were killed by cervical dislocation 24 h after injection. Ten micrograms of total RNA per lane was hybridized with the appropriate mouse cDNA probes (25).

RT-PCR Analyses of hAHR and Murine Ahr mRNA Expression in Embryos. Total RNA was isolated from palate and kidney of gestation day (GD)18.5 fetus by using ISOGEN. One microgram of

the total RNA was reverse-transcribed into cDNA with Superscript-II reverse transcriptase (Life Technologies, Gaithersburg, MD) and random hexamers at 42°C for 50 min. The resulting cDNAs were subjected to 30 cycles of PCR by using the specific primers for the gene for the h*AHR* (5' primer, 5'-GTAAGTCTC-CCTTCATACC-3'; 3' primer, 5'-AGGCACGAATTGGTTA-GAG-3'), mouse *Ahr* (5' primer, 5'-CTTTGCTGAACTCGGCT-TGC-3'; 3' primer, 5'-TTGCTGGGGGCACACCATCT-3') and GAPDH (5' primer, 5'-CCCCTTCATTGACCTCAACTA-CATGG-3'; 3' primer, 5'-GCCTGCTTCACCACCTTCTTGAT-GTC-3'). The reaction was performed under the following conditions: 94°C for 30 sec, 60°C for 30 sec, and 72°C for 30 sec.

Immunohistochemical Analysis of hAHR Expression. Immunohistochemical analysis was performed as described (26). Lungs were fixed in 0.1 M phosphate buffer containing 4% paraformaldehyde for 24 h and embedded in paraffin. Sections were incubated with anti-AHR antibody in 1:200 dilution, which reacts with both human and mouse AHR (N-19; Santa Cruz Biotechnology). AHR immunoreactivity was visualized with the avidin-biotin-peroxidase system (Vector Laboratories).

TCDD Treatment and Evaluation of Teratogenesis. TCDD treatment was performed as described (22). On GD12.5, pregnant mice were given TCDD by i.p. administration at a dose of 40 μg/kg body weight (27). On GD18.5, the fetuses were taken out and fixed in 4% paraformaldehyde. The palatal structure was examined by cutting between the upper and lower jaws. The kidneys were sliced longitudinally and stained with hematoxylin/eosin. The presence and severity of hydronephrosis in each kidney was examined under a microscope as previously described (28) by using severity scores ranging from 0 to 3+ (0, normal kidney; 1+, slight decrease in length of papilla; 2+, marked decrease in length of papilla with some loss of renal parenchyma; 3+, complete absence of papilla, shell of kidney remaining with only a small amount of renal parenchyma). For statistical analysis, pairwise comparisons were made by Mann–Whitney U test, by using StatView for Macintosh version 5.0 (SAS Institute, Cary, NC).

Results

Replacement of the Mouse *Ahr* Gene with hAHR cDNA. We hypothesize that the specific functional characteristics of the hAHR molecule form the principal basis for the pattern of human responses to xenobiotics that interact with the AHR. To characterize responses mediated by hAHR, we generated a mouse possessing hAHR instead of murine AHR. hAHR cDNA was introduced into the mouse *Ahr* locus by homologous recombination, thereby disrupting the mouse *Ahr* gene (Fig. 1A). The cDNA was recombined so that hAHR is expressed under the control of the endogenous mouse *Ahr* promoter. Sixteen independent G418-resistant ES clones were obtained of 240 by PCR screening, and seven clones were further confirmed as correctly targeted ES cells by genomic DNA blot analysis. *Eco*RI-digested genomic DNA from the three representative positive clones (nos. 14, 25, and 58) revealed 11.0- and 6.2-kb fragments derived from the intact and targeted alleles, respectively, when hybridized with the 5'-external probe (Fig. 1B).

These three clones harboring h*AHR* were used for the generation of chimeric offspring. The male chimeras were mated with C57BL/6J females to obtain heterozygotes of the h*AHR* allele. They were subsequently bred into a C57BL/6J genetic background through the seventh generation, and the backcrossed heterozygous animals were interbred to yield hAHR homozygous mutant mice. The transmission of the targeted allele to the offspring was confirmed by genomic DNA blot analysis, and the genotype was determined by PCR by using tail DNA as a template (Fig. 1 C and D). Of 124 offspring obtained
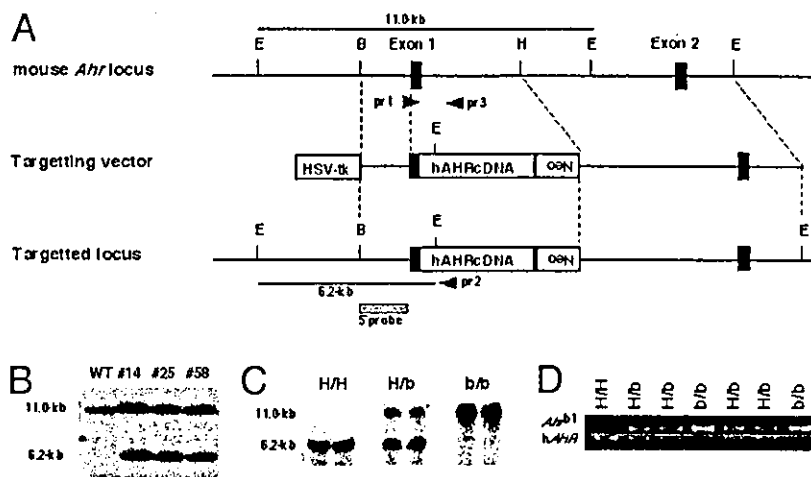
Fig. 1. Generation of the hAHR knock-in mouse. (A) Strategy for hAHR cDNA knock-in by homologous recombination. E, H, and B are restriction sites for EcoRI, HindIII, and BamHI, respectively. Neo indicates the neomycin-resistance gene, and HSV-tk is the thymidine kinase gene under control of the herpes simplex virus promoter. The 5′-genomic probe used for DNA blot analysis is indicated by the hatched box. The positions of wild-type (pr 3) and mutant allele-specific (pr 2) primers and the common primer (pr 1) used in the genotyping PCR are indicated by arrowheads. The EcoRI restriction fragments detected with the 5′-genomic probe in the wild-type and targeted allele are denoted by horizontal bars. (B) DNA blot analyses of three recombinant ES clones. Genomic DNA was prepared from the ES clones (nos. 14, 25, and 58), and aliquots (10 μg) were digested by EcoRI. EcoRI digestion generated 11.0- and 6.2-kb bands for the wild-type and targeted alleles, respectively, by using the 5′-genomic probe. (C) Genotyping of the Ahr gene by DNA blot analysis. Genomic DNA was extracted from the tails of heterozygous and homozygous hAHR mice and wild-type Ahr$^{b-1/b-1}$ mice and digested by EcoRI for DNA blot analysis. (D) Genotyping of littermates from the intercrosses of heterozygotes. PCR fragments of wild-type amplified with pr1 and pr3 (Ahr^{b-1}; 280 bp) and mutant allele with pr1 and pr2 (hAHR; 240 bp) as depicted in A. H/H, H/b, and b/b indicate homozygous and heterozygous hAHR mice and wild type (Ahr$^{b-1/b-1}$), respectively.

from heterozygous matings, wild-type (Ahr$^{b-1/b-1}$), heterozygous, and homozygous hAHR mutant mice numbered 29, 71, and 24, respectively, conforming to the expected Mendelian inheritance ratio. Homozygous hAHR mice were viable, and no abnormalities were observed.

Expression of hAHR in hAHR Knock-in Mice. The expression of hAHR and mouse Ahr mRNAs was examined by RNA blot analysis by using polyA RNAs isolated from major AHR-expressing organs including liver, lung, kidney, intestine, and thymus (Fig. 2A). A cDNA fragment encoding the PAS domain of C57BL/6 AHR, which shows 83% homology with the corresponding human molecule, was used as a common probe for detecting both mouse Ahr and hAHR mRNAs. The larger band detected in heterozygous hAHR mice and wild-type Ahr$^{b-1/b-1}$ mice corresponds to the 5.4-kb transcript derived from the endogenous Ahr^{b-1} gene, and the shorter 5.0-kb transcript observed in heterozygous and homozygous hAHR is derived from the hAHR knock-in allele. This result establishes that, whereas the homozygous hAHR mouse lacks mRNA for murine Ahr, it expresses mRNA for hAHR. Further, the level of expression of hAHR mRNA is comparable to that of endogenous murine Ahr mRNA in the other strains.

The embryonic expressions of mouse Ahr and hAHR mRNAs were examined by RT-PCR at the stage of GD18.5. As observed in the RNA blot analysis of adult tissues, the hAHR mRNA was expressed in the embryonic palate and kidney of homozygous and heterozygous hAHR mice. The abundance was comparable with that of the mouse Ahr mRNA expressed in Ahr$^{b-1/b-1}$ and heterozygous hAHR mice (Fig. 2B). These results demonstrate that hAHR mRNA is transcribed under the control of the mouse Ahr promoter in both adult and embryonic hAHR knock-in mice.

To ascertain that hAHR protein is expressed from the knock-in allele, immunohistochemical analysis was performed on lung sections obtained from hAHR knock-in homozygous mouse and the Ahr-null mutant (22). Intense signals were detected in the alveolar epithelial cells of hAHR knock-in animals (Fig. 2C). The signal

intensity of Ahr-null mutant lung (Fig. 2D) was as faint as the hAHR knock-in lung without the antibody (data not shown). Thus, hAHR protein is expressed from the knock-in allele.

The hAHR Knock-in Mouse Displays a Distinct Induction Profile of AHR Target Genes to Different AHR Ligands. The response of the hAHR knock-in mouse to two prototypical AHR ligands, 3-MC and TCDD, was examined. To characterize the distinct properties, if any, of the hAHR, two strains of control mice were used for the analysis. One strain is a wild-type mouse in the C57BL/6J genetic background, which possesses AHR with high affinity for TCDD. The other strain is a congenic mouse, D2N-Ahr^d, possessing AHR with low affinity (from DBA/2 mouse) in the C57BL6J genetic background. Because the hAHR knock-in mouse was backcrossed into C57BL/6J, these two strains of mouse enabled us to compare the characteristics of hAHR to those of C57BL/6J and DBA/2 AHR in the same genetic background.

Robust expression of the CYP1A1 and CYP1A2 genes was observed in the liver of Ahr$^{b-1/b-1}$ mice after administration of 3-MC, whereas the magnitudes of induction in homozygous hAHR and Ahr$^{d/d}$ mice were much weaker and comparable to each other (Fig. 3A). The relative mean band intensities for CYP1A1 were 1.0 and 0.9 and were 1.0 and 1.1 for CYP1A2 in homozygous hAHR and Ahr$^{d/d}$ mice, respectively. After treatment with TCDD, the induction of the two genes was strongest in Ahr$^{b-1/b-1}$ mice, intermediate in Ahr$^{d/d}$ mice, and weakest in homozygous hAHR mice (Fig. 3B). The fold inductions in homozygous hAHR, Ahr$^{d/d}$, and Ahr$^{b-1/b-1}$ mice were 1.0, 4.9, and 14.6 for CYP1A1, and 1.0, 5.7, and 8.4 for CYP1A2, respectively.

When the responses of Ahr$^{b-1/b-1}$ and Ahr$^{d/d}$ mice were compared, the CYP1A1 expression levels were higher in Ahr$^{b-1/b-1}$ than in Ahr$^{d/d}$ mice, which is consistent with previous reports (9, 12, 13). It is noteworthy that the responsiveness of homozygous hAHR mice to 3-MC was almost comparable to that of Ahr$^{d/d}$ mice, whereas the responsiveness to TCDD was much weaker. The differential response between Ahr$^{d/d}$ and homozygous hAHR mice was unexpected, because a previous study indicated

A

	lung			live			kidney		
	H/H	H/b	b/b	H/H	H/b	b/b	H/H	H/b	b/b

Ahr^b
hAHR
GAPDH

	intestine			thymus		
	H/H	H/b	b/b	H/H	H/b	b/b

Ahr^b
hAHR
GAPDH

B

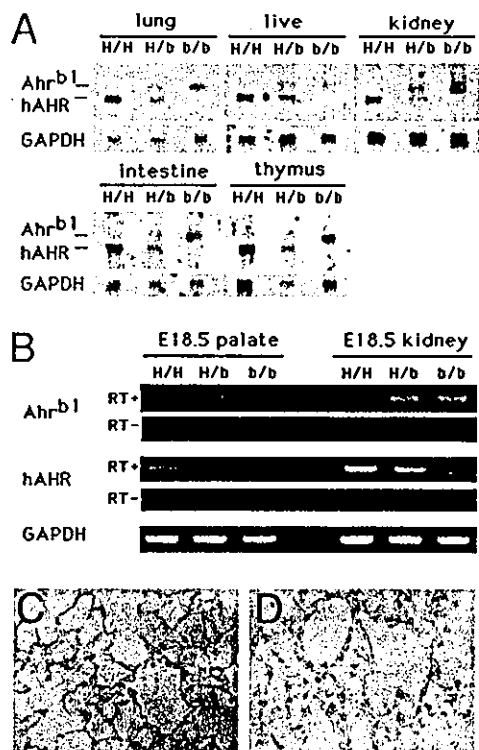|		E18.5 palate			E18.5 kidney		
		H/H	H/b	b/b	H/H	H/b	b/b

Ahr^b   RT+ / RT−

hAHR   RT+ / RT−

GAPDH

Fig. 2. Expression of hAHR in multiple tissues of the hAHR knock-in mouse. (A) RNA blot analysis of polyA RNA (5 μg/lane) extracted from five representative organs of homozygous and heterozygous hAHR mice and Ahr^b-1/b-1 mice. Human and mouse Ahr transcripts (hAHR and Ahr^b-1, respectively) are indicated (Left). The same membrane was rehybridized with ³²P-labeled cDNA of mouse GAPDH. H/H, H/b, and b/b are described in the Fig. 1 legend. (B) RT-PCR analyses of hAHR and murine Ahr mRNA expression in kidney and palate of GD18.5 fetuses. The reverse transcription was conducted either in the presence (+) or absence (−) of reverse transcriptase. PCR products representing the transcripts derived either from hAHR or Ahr^b-1 are indicated on the left. (C and D) Immunohistochemical analysis of hAHR protein in the lung of a homozygous hAHR mouse. Immunoreactivity of AHR protein was observed in the alveolar epithelial cells of homozygous hAHR lung (C), whereas no immunoreactivity was observed in the lung of Ahr^−/− mouse (D). Original magnifications, ×400 (C and D).

that hAHR and DBA/2 AHR exhibit similar dissociation constants for TCDD binding as measured in vitro (9, 19). This result suggests that ligand binding does not fully define the integrated function of hAHR.

hAHR Knock-in Mouse Is Relatively Resistant to TCDD-Induced Teratogenicity. The responses to TCDD mediated by hAHR are weaker than that by DBA/2 and C57BL/6 AHR when measured
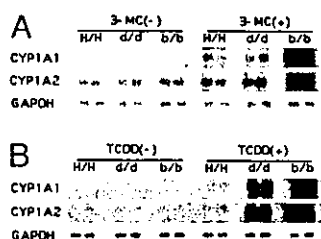

A 3-MC(−) / 3-MC(+)

	H/H	d/d	b/b	H/H	d/d	b/b
CYP1A1						
CYP1A2						
GAPDH						

B TCDD(−) / TCDD(+)

	H/H	d/d	b/b	H/H	d/d	b/b
CYP1A1						
CYP1A2						
GAPDH						

Fig. 3. Inducible expression of AHR target genes. Northern blot analysis of AHR-regulated CYP1A1 and CYP1A2 was performed. Six-week-old homozygous hAHR, Ahr^d/d, and Ahr^b-1/b-1 mice were treated with 80 mg/kg 3-MC (A) or 100 μg/kg TCDD (B). Total hepatic RNA was isolated 24 h after treatment and subjected to Northern analysis (10 μg/lane). Equal loading was confirmed by the abundance of GAPDH transcripts.
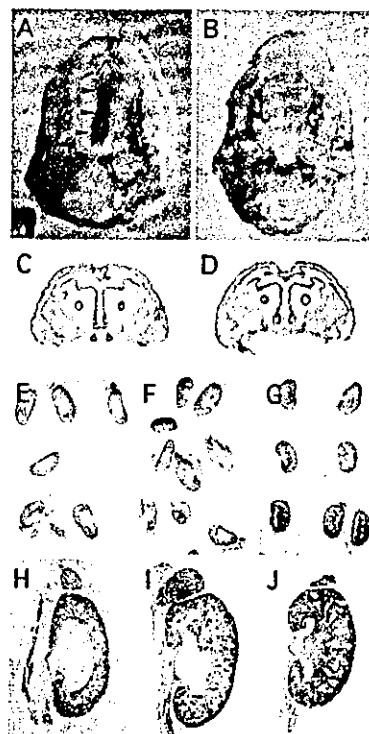

Fig. 4. Fetal teratogenesis after maternal administration of TCDD. (A and C) Cleft palate in an Ahr^b-1/b-1 fetus is shown. Filled arrowheads in A and open arrowheads in C indicate the failure of palatine shelves to fuse. Note that homozygous hAHR fetuses showed no cleft palates after TCDD treatment (B and D). (E, F, H, and I) Fetal hydronephrosis induced by TCDD. Ahr^b-1/b-1 (E and H) and homozygous hAHR (F and I) fetuses are shown. (G and J) Unaffected kidneys from untreated Ahr^b-1/b-1 fetuses are shown.

as inducibility of *CYP1A* family genes. Teratogenicity is a more integrated and complex toxicological manifestation of TCDD action. The most prominent teratogenic effects of TCDD on mouse fetus are cleft palate and hydronephrosis, both of which depend completely on AHR expression (29). The frequency and severity of these teratogenic effects of TCDD were examined in hAHR knock-in fetuses. Homozygous hAHR knock-in females were mated with males of the same genotype and given a single i.p. dose of 40 μg of TCDD per kg of body weight at GD12.5. Ahr^b-1/b-1 and Ahr^d/d females were treated in the same way as controls. All dams were weighed to monitor the normal continuation of the pregnancy and killed at GD18.5 to remove fetuses for examination of cleft palate and hydronephrosis.

As reported previously, cleft palate was observed in 100% of the wild-type Ahr^b-1/b-1 fetuses exposed to TCDD (Fig. 4 A and C and Table 1) (22). By contrast, none of the treated homozygous hAHR fetuses showed abnormal palatogenesis (Fig. 4 B and D and Table 1). An intermediate frequency (30%) of cleft palate was observed in the Ahr^d/d fetuses. Differences in the severity of cleft palate were not apparent in any of the symptomatic fetuses of any genotype. This anomaly was most frequent in Ahr^b-1/b-1, intermediate in Ahr^d/d, and least frequent in homozygous hAHR mice, in accordance with the transcriptional inducibility of AHR target genes, which was strongest in Ahr^b-1/b-1, intermediate in Ahr^d/d, and weakest in homozygous hAHR mice. Thus, a strong correlation between the incidence of cleft palate in each strain and the intrinsic transcriptional activity of their respective AHR molecules was observed.

Hydronephrosis, another teratogenic effect of TCDD, is characterized by a dilated renal pelvis. The severity of this anomaly in the fetal kidney was scored from 0 (normal) to 3 (severest)

Moriguchi et al.

446

Table 1. Incidence of anomalies caused by TCDD in homozygous hAHR, $Ahr^{b-1/b-1}$, and $Ahr^{d/d}$ fetuses

Genotype of fetuses	TCDD dose, μg/kg	Dams examined, n	Fetuses examined, n	Cleft palate		Hydronephrosis		
				n	%*	n	%*	Severity: 0–3.0†
$Ahr^{b-1/b-1}$	0	2	13	0	0	2	12.5	0.19 ± 0.10‡
$Ahr^{b-1/b-1}$	40	5	29	29	100	26	89.7	2.54 ± 0.14§
$Ahr^{d/d}$	0	2	15	0	0	2	13.3	0.20 ± 0.10‡
$Ahr^{d/d}$	40	5	30	9	30	25	81.7	1.98 ± 0.14§
Homo-hAHR	0	2	16	0	0	1	6.3	0.03 ± 0.03‡
Homo-hAHR	40	5	37	0	0	30	81.1	1.19 ± 0.01§

*Percentage of fetuses with each anomaly of all fetuses examined.
†The criteria for severity scores are described in Materials and Methods. Data are expressed as mean ± SE.
‡Significant difference between TCDD-treated and -untreated fetuses of each genotype ($P < 0.0001$).
§Significant difference between TCDD-treated homozygous hAHR fetuses and $Ahr^{b-1/b-1}$ or $Ahr^{d/d}$ fetuses ($P < 0.0001$).

according to criteria described previously (28). When kidneys scored at 1, 2, or 3 were counted as hydronephrotic, 89.7% of the $Ahr^{b-1/b-1}$ offspring suffered from this teratogenic outcome after TCDD treatment (Fig. 4 E and H, and Table 1 for TCDD-treated animals; Fig. 4 G and J, and Table 1 for untreated animals). A similar incidence was observed in a previous study (22). $Ahr^{d/d}$ and homozygous hAHR fetuses also displayed this teratogenic effect with incidences of 81.7% and 81.1%, respectively (Fig. 4 F and I, and Table 1). Thus, there is no substantial difference in the incidence of hydronephrosis among the mice expressing the three distinct Ahr (hAHR) genes. When severity score values were compared among the TCDD-treated fetuses, they averaged 2.54, 1.98, and 1.19 for the $Ahr^{b-1/b-1}$, $Ahr^{d/d}$ and homozygous hAHR genotypes, respectively (Table 1). Therefore, hydronephrosis observed in the homozygous hAHR fetuses was significantly less severe compared with that in either $Ahr^{b-1/b-1}$ or $Ahr^{d/d}$ fetuses. Nonetheless, the average score of TCDD-treated homozygous hAHR fetuses (1.19) was still significantly higher than that of untreated homozygous hAHR fetuses (0.03), clearly demonstrating that the TCDD-activated hAHR mediates renal teratogenesis in mice. Although the magnitude of CYP gene induction is dramatically different depending on the Ahr genotype, the incidence of hydronephrosis is surprisingly comparable among the three strains. These results revealed that differences between human and murine AHR allowed for the emergence of discrete biological effects; e.g., hydronephrosis, but not cleft palate in homozygous hAHR mice.

To exclude the possibility that maternal factors affect the teratogenic manifestations on the fetuses, heterozygous hAHR parents were used to obtain homozygous hAHR and $Ahr^{b-1/b-1}$ fetuses. Heterozygous mothers were treated with TCDD as described above, and fetuses were examined for both cleft palate and hydronephrosis. As described in Table 2, the incidence of cleft palate was 100% and 0% in $Ahr^{b-1/b-1}$ and homozygous hAHR fetuses, respectively, which is identical to the results presented in Table 1. The incidence and severity (mean score)

of hydronephrosis were 100% and 2.47 for $Ahr^{b-1/b-1}$ and 66.6% and 1.17 for homozygous hAHR fetuses, respectively. Again, a more moderate effect in the homozygous hAHR fetuses is suggested, the severity difference being statistically significant. Therefore, we conclude that the TCDD-induced teratogenic effects are independent of maternal genotypes, and that fetal AHR activity is critical for determining the outcomes.

Discussion

One of the central issues in the uncertainty surrounding risk assessments for TCDD and its structural analogs is whether humans are relatively sensitive or resistant to the toxicities of this class of compounds. Because the pleiotropic adverse effects induced by these toxins involve multiple processes, the human response is generated by the summation and integration of the properties inherent to the human components, including expression level, ligand-binding affinity, and transcriptional activity of the AHR, as well as the variety, function and activity of the AHR target genes. Through numerous preceding studies, the primary structure of the AHR protein has been regarded as one of the most critical factors determining the susceptibility and specificity of responses of animals to various PAH/HAHs including dioxin. On the basis of several observations in vitro, polymorphic variation in the Ahr gene is considered the primary basis for differences in sensitivity to TCDD among strains of mice (9–11). In this study, we attempted to establish an in vivo system to evaluate the specific function of the hAHR protein to better evaluate its role in determining possible patterns of human responses to PAH/HAHs.

For this purpose, we adopted a knock-in strategy to introduce hAHR cDNA into the mouse Ahr genomic locus by homologous recombination. This strategy offers an obvious advantage compared with a transgenic method, because the introduced sequence is transcribed under the same regulatory mechanisms the replaced gene (30). As desired, expression levels of the hAHR transcript were almost the same with those of endogenous mouse

Table 2. Incidence of anomalies caused by TCDD in fetuses from heterozygous hAHR parents

Genotype of fetuses	TCDD dose, μg/kg	Dams examined, n	Fetuses examined, n	Cleft palate		Hydronephrosis		
				n	%*	n	%*	Severity: 0–3.0
$Ahr^{b-1/b-1}$	40		9	9	100	9	100.0 •	2.47 ± 0.14†
Hetero-hAHR	40	7	25	12	48	22	88.0	2.46 ± 0.13
Homo-hAHR	40		12	0	0	8	66.6	1.17 ± 0.01†

*Percentage of fetuses with each anomaly out of all fetuses examined.
†Significant difference between homozygous hAHR and $Ahr^{b-1/b-1}$ fetuses ($P < 0.0001$).

447

Ahr mRNA in multiple AHR-expressing tissues of adult mice and GD18.5 embryos. The hAHR· protein was detected by immunostaining in the lungs of homozygous h*AHR* mice.

A possible explanation of the relative resistance of the hAHR knock-in mouse to TCDD lies in the qualitative difference between the human and mouse AHR molecules. Assuming that the abundance of the hAHR protein is the same as that of the endogenous mouse AHR, our results imply that the hAHR-mediated response to TCDD *in vivo* is much lower than that of DBA/2 AHR, although previous reports showed that their affinities to TCDD, as measured *in vitro*, are almost the same (9, 19). Alignment of the primary amino acid sequences of the two molecules indicates the considerable divergence in the C-terminal regions (9) and the deletion analysis differently localized the transcriptional activity within the regions (31). Such structural diversity of the C-terminal region might lead to species-specific interaction behaviors with transcriptional cofactors. TCDD-activated hAHR may not recruit coactivators as efficiently as the DBA/2 counterpart. One possibility must be noted that the incompatibility between TCDD-activated hAHR and the mouse coactivators may cause the reduced response of hAHR knock-in mouse to TCDD.

hAHR was not detectable by immunoblot analysis with the current antiserum, and its abundance relative to the constitutive level of mouse AHR protein could not be determined. Considering this lack of quantitative information, limited protein accumulation might account for the attenuated responsiveness of hAHR knock-in mice to TCDD. hAHR may have an intrinsically shorter life than mouse AHR at physiological expression levels *in vivo*.

The susceptibility of embryonic kidneys of homozygous h*AHR* mice to the teratogenic effects of TCDD is noteworthy. The pathogenesis of this renal lesion induced by TCDD involves hyperplasia of the ureteric epithelium, resulting in an occlusion of the ureter and subsequent hydronephrosis (32). Adverse effects on the kidney and urinary tract have also been reported in humans exposed to TCDD (33). However, studies in Ben Tre Province in Vietnam, where defoliant containing dioxin was sprayed extensively, revealed little increase in the prevalence of cleft lip and/or

palate compared with that observed in Japan (34), suggesting that hAHR is less potent to mediate the manifestation of cleft palate, and that a higher dose might be required for it. Consistent with these human reports, our analysis showed that hAHR, although expressed in mice, mediated the development of hydronephrosis induced by TCDD, but not cleft palate at our experimental dose. Thus, the knock-in animal seems·to mimic some aspects of the human responses to PAH/HAHs.

An intriguing utilization of our knock-in mouse strategy would be as an *in vivo* system for the qualitative and quantitative assessment of possible human responses to various PAH/HAHs. In this study, D2N-*Ahrd* mice responded more strongly to TCDD ·than to 3-MC, whereas the hAHR knock-in mice responded almost equally to these two compounds. These results clearly show that the relative efficacy profiles, examined by TCDD and 3-MC, are different between D2N-*Ahrd* and our hAHR knock-in mouse. Therefore the efficacy profile specific to hAHR can be displayed by analyses of the responses of the hAHR knock-in mouse to an array of PAH/HAHs. Because environmentally relevant levels of exposure to dioxin and related compounds have garnered much concern in terms of their possible effects on reproductive, neurobehavioral, and immunological functions of humans, our hAHR knock-in mouse will serve as a humanized model mouse, exhibiting the human-specific responses to PAH/HAH congeners. This mouse should help define the range of biological and toxicological effects that could be expected to affect humans and thereby reduce some uncertainty in risk assessments of these persistent environmental contaminants.

1. Poland, A. & Knutson, C. (1982) *Annu. Rev. Pharmacol. Toxicol.* 22, 517–554.
2. Whitelock, J. P., Jr. (1990) *Annu. Rev. Pharmacol. Toxicol.* 30, 251–277.
3. Landers, J. P. & Bunce, N. J. (1991) *Biochem. J.* 276, 273–287.
4. Swanson, H. J. & Bradfield, C. A. (1993) *Pharmacogenetics* 3, 213–230.
5. Hoffman, E. C., Reyes, H., Chu, F.-F., Sander, F., Conly, L. H., Brooks, B. A. & Hankinsin, O. (1991) *Science* 252, 954–958.
6. Okey, A. B., Riddick, D. & Harper, P. A. (1994) *Toxicol. Lett.* 70, 1–22.
7. Rowlands, J. & Gustafsson, J. A. (1997) *CRC Crit. Rev. Toxicol.* 27, 109–134.
8. Poellinger, L. (2000) *Food Addit. Contam.* 17, 261–266.
9. Ema, M., Ohe, N., Suzuki, M., Mimura, J., Sogawa, K., Ikawa, S. & Fujii-Kuriyama, Y. (1994) *J. Biol. Chem.* 269, 27337–27343.
10. Poland, A. & Glover, E. (1990) *Mol. Pharmacol.* 38, 306–312.
11. Poland, A., Palen, D. & Glover, E. (1994) *Mol. Pharmacol.* 46, 915–921.
12. Ema, M., Matsushita, N., Sogawa, K., Ariyama, T., Inazawa, J., Nemoto, T., Ota, M., Oshimura, M. & Fujii-Kuriyama, Y. (1994) *J. Biochem.* 116, 845–851.
13. Dolwick, K. M., Schmidt, J. V., Carver, L. A., Swanson, H. I. & Bradfield, C. A. (1993) *Mol. Pharmacol.* 44, 911–917.
14. Okey, A. B., Vella, L. M. & Harper, P. A. (1989) *Mol. Pharmacol.* 35, 823–830.
15. Pohjanvirta, R., Unkila, M. & Tuomisto, J. (1993) *Pharmacol. Toxicol.* 73, 52–56.
16. Pohjanvirta, R., Wong, J. M. Y., Li, W., Harper, P. A., Tuomisto, J. & Okey, A. B. (1998) *Mol. Pharmacol.* 54, 86–93.
17. Tuomisto, J. T., Viluksela, M., Pohjanvirta, R. & Tuomisto, J. (1999) *Toxicol. Appl. Pharmacol.* 155, 71–81.
18. Mocarelli, P., Gerthoux, P. M., Ferrari, E., Patterson, D. G., Jr., Kieszak, S. M., Brambilla, P., Vincoli, N., Signorini, S., Tramacre, P., Carreri, V., *et al.* (2000) *Lancet* 355, 1858–1863.
19. Micka, J., Milatovich, A., Menon, A., Grabowski, G. A., Puga, A. & Nebert, D. W. (1997) *Pharmacogenetics* 7, 95–101.
20. Kohkalainen, M., Tuomisto, J. & Pohjanvirta, R. (2001) *Biochem. Biophys. Res. Commun.* 285, 1121–1129.

21. Abnet, C. C., Tanguay, R. L., Heideman, W. & Peterson, R. E. (1999) *Toxicol. Appl. Pharmacol.* 159, 41–51.
22. Mimura, J., Yamashita, K., Nakamura, K., Morita, M., Takagi, T. N., Nakao, K., Ema, M., Sogawa, K., Yasuda, M., Katsuki, M., *et al.* (1997) *Genes Cell.* 2, 645–654.
23. Hooper, M., Hardy, K., Handyside, A., Hunter, S. & Monk, M. (1987) *Nature* 326, 292–295.
24. Ema, M., Sogawa, K., Watanabe, N., Chujoh, Y., Matsushita, N., Gotoh, O., Funae, Y. & Fujii-Kuriyama, Y. (1992) *Biochem. Biophys. Res. Commun.* 184, 246–253.
25. Fernandez-Salguero, P., Pineau, T., Hilbert, D. M., McPhail, T., Lee, S. S. T., Kimura, S., Nebert, D. W., Rudikoff, S., Ward, J. M. & Gonzalez, F. J. (1995) *Science* 268, 722–726.
26. Moriguchi, T., Sakurai, T., Takahashi, S., Goto, K. & Yamamoto, M. (2002) *J. Biol. Chem.* 277, 16985–16992.
27. Yasuda, M., Igarashi, E., Datu, A. R. & Igawa, H. (1986) *Teratology* 34, 454–455.
28. Birnbaum, L. S., Harris, M. W., Barnhart, E. R & Morrissey, R. E. (1987) *Toxicol. Appl. Pharmacol.* 90, 206–216.
29. Birnbaum, L. S. & Abbott, B. (1997) in *Methods in Developmental Toxicology and Biology*, eds. Klug, S. & Thiel, R. (Blackwell Science, London), pp. 51–63.
30. Tsai, F. Y., Browne, C. P. B. & Orkin, S. H. (1998) *Dev. Biol.* 196, 218–227.
31. Kumar, M. B., Ramadoss, P., Reen, R. K., Vanden Heuvel, J. P. & Perdew, G. H. (2001) *J. Biol. Chem.* 276, 42302–42310.
32. Hoffman, R. E., Stehr-Green, P. A., Webb, K. B., Evans, R. G., Knutson, A. P., Schramm, W. F., Staak, J. L., Gibson, B. B. & Steinberg, K. K. (1986) *J. Am. Med. Assoc.* 255, 2031–2038.
33. Abbott, B. D., Birnbaum, L. S. & Pratt, R. M. (1987) *Teratology* 35, 329–334.
34. Natsume, N., Kawai, T. & Le, H. (1998) *Cleft Palate Craniofac. J.* 35, 183–185.

448

A novel induction mechanism of the rat *CYP1A2* gene mediated by Ah receptor–Arnt heterodimer☆,☆☆,★

Kazuhiro Sogawa,[a,*] Keiko Numayama-Tsuruta,[a,1] Tomohiro Takahashi,[a]
Natsuki Matsushita,[a,2] Chisa Miura,[a] Jun-ichi Nikawa,[b] Osamu Gotoh,[c] Yasuo Kikuchi,[a]
and Yoshiaki Fujii-Kuriyama[a,3]

[a] *Department of Biomolecular Science, Graduate School of Life Sciences, Tohoku University, Aoba-ku, Sendai 980-8578, Japan*
[b] *Department of Biochemical Engineering and Science, Faculty of Computer Science and Systems Engineering, Kyushu Institute of Technology,
Iizuka, Fukuoka 820-8502, Japan*
[c] *Department of Intelligence Science and Technology, Graduate School of Informatics, Kyoto University, Kyoto 606-8501, Japan*

Received 14 April 2004
Available online 6 May 2004

Abstract

We have identified an enhancer responsible for induction by 3-methylcholanthrene in the upstream region of the *CYP1A2* gene. The enhancer does not contain the invariant core sequence of XREs that are binding sites for the Ah receptor (AhR) and Arnt heterodimer. The enhancer did not show any inducible expression in Hepa-1-derived cell lines, C4 and C12, deficient of Arnt and AhR, respectively. On the other hand, bacterially expressed AhR–Arnt heterodimer could not bind to the enhancer. Mutational analysis of the enhancer revealed that a repeated sequence separated by six nucleotides is important for expression. A factor binding specifically to the enhancer was found by using gel shift assays. Bacterially expressed AhR–Arnt heterodimer interacted with the factor. A dominant negative mutant of the AhR to XRE activated the enhancer. Collectively, these results demonstrate that a novel induction mechanism is present in which the AhR–Arnt heterodimer functions as a coactivator.
© 2004 Elsevier Inc. All rights reserved.

Keywords: CYP1A2; Coactivator; Inducible expression; Xenobiotic response; Ah receptor; Arnt; Enhancer

The cytochrome P450 (CYP) monooxygenases are a group of proteins responsible for the oxidation of drugs, environmental pollutants, and endogenous compounds such as steroids and fatty acids [1]. CYP1A2 is an inducible drug-metabolizing P450 and biotransforms foreign chemicals, especially carcinogenic heterocyclic amines such as 2-amino-3,8-dimethylimidazo[4,5-*f*]quinoxaline (MeIQx) and 2-amino-1-methyl-6-phenylimidazo[4,5-*b*]pyridine (PhIP), which are formed in meat and fish during cooking [2]. CYP1A2 is expressed preferentially in the liver [3]. However, other extrahepatic tissues such as the lung [4], esophagus [5], and brain [6] have been reported to express CYP1A2. Two different groups of inducers are known to induce CYP1A2. One includes various man-made chemicals such as 3-methylcholanthrene (MC) and 2,3,7,8-tetrachlorodibenzo-*p*-dioxin (TCDD) which act as ligands for the Ah receptor (AhR), a ligand-activated transcription factor [7,8].

These inducers also induce a number of other drug-metabolizing enzymes such as CYP1A1, glutathione S-transferase Ya subunit, and a form of UDP-glucuronosyltransferase [7,8]. The other is CYP1A2-specific inducers represented by isosafrole [9]. Reports have indicated that induction of CYP1A2 by MC was caused partly by an increased transcription rate and partly by increased stabilization of the mRNA [10,11]. Recent studies, however, on mice lacking the AhR gene clearly demonstrate that the AhR is indispensable for the inducible expression of CYP1A2 as well as CYP1A1, and accordingly enhanced transcription of the *CYP1A2* gene is predominantly important for the induction, although the possibility cannot be ruled out that the AhR is involved in stabilization of the *CYP1A2* mRNA [12,13].

The stimulated AhR with inducers forms a heterodimer with Ah receptor nuclear translocator (Arnt) in the nucleus after dissociation from Hsp90, and activates transcription of its target genes by binding xenobiotic responsive element (XRE) localized in their control region [7,8]. XRE contains an invariant CACGC core sequence that is recognized by the AhR and Arnt heterodimer [14,15], and is known to be present in most, if not all, of MC-inducible genes hitherto examined ([7,8] and references therein).

In this paper, we describe a novel enhancer element in the upstream region of the rat *CYP1A2* gene which responds to stimulus by MC. The enhancer does not contain the XRE core sequence but contains a short repeated sequence conferring the inducibility to the gene. Furthermore, we present evidence that the factor which recognizes and binds the repeated sequence recruits the AhR–Arnt complex by interacting with it.

Materials and methods

Construction of plasmids. pIS-5600, containing a 6.7 kb genomic DNA fragment spanning from −5.6 kb upstream of the transcription-initiation site to the initiation codon (+1100) in the 2nd exon, was constructed from pMLCAT [16] and the *CYP1A2* gene [17]. Plasmids with various deletions were constructed by using Bal 31 exonuclease. These various deletion plasmids were designated as pIS-x (x indicates the length of the 5′ flanking sequence of the *CYP1A2* gene from the transcription-initiation site). pIS-2237x was constructed by converting the *Sph*I site (at the −2085 position) into the *Xho*I site with a synthetic linker. Various DNA fragments from the *CYP1A2* gene were inserted into the *Cla*I site of pMC53c which contains the *CYP1A1* promoter [18], and designated pMCD-x or pMCD-xr (x indicates the length of the 5′ upstream sequence of the *CYP1A2* gene from the transcription-initiation site, and r indicates reverse orientation). pGL3 promoter plasmid (Promega, Madison) was cleaved with *Bgl*II, and synthetic oligonucleotides for the two copies of sequences shown in Fig. 5 were inserted. For expression in cultured cells, human AhR and Arnt cDNAs were inserted in the *Xho*I site of pEFBOS vector [19]. To construct an expression plasmid for a dominant negative mutant of the AhR, AGA for Arg 39 in the basic sequence was changed to ATA for Ile by using synthetic oligonucleotides. For expression in yeast, human AhR and Arnt cDNAs were inserted in the *Eco*RI site (artificially

generated using a synthetic linker) of pGAD424 (Clontech, Palo Alto) in which a sequence for activation domain of GAL4 and nuclear localization signal (*Xmn*I to *Bam*HI site) had been removed beforehand. A selection marker, LEU2, of Arnt expression plasmid was changed to TRP1. Reporter plasmids containing the *CYP1A2* enhancer or XRE or HRE [20] were constructed by inserting the corresponding synthetic oligonucleotides into the *Sma*I site of pZ7 [21] containing promoter of the yeast myo-inositol transporter 1 gene and the β-galactosidase gene. All constructions were confirmed by sequencing.

Cell culture, DNA transfection, and reporter assays. HepG2, Hepa-1, C4, and C12 cells were maintained as described [22,23]. The calcium phosphate precipitation method was employed for transfection as described [24]. Each of the test plasmids (5 μg) containing the CAT reporter gene was introduced into cultured cells with 1 μg of a plasmid consisting of the luciferase gene as an internal control for efficiency of transfection. The CAT assay was performed as described [25]. When the luciferase gene was used as the reporter, β-galactosidase-expression plasmid was used as an internal control for efficiency of transfection. All experiments were done at least 3 times.

Gel mobility shift analysis. Nuclear extracts were prepared from HepG2 cells grown in the presence or absence of 1 μM MC for 2 h by the method of Dignam et al. [26]. Gel mobility shift assays were performed as described [27].

Expression of AhR and Arnt in Escherichia coli and yeast. Chimeric proteins containing basic helix–loop–helix (bHLH) and PAS domains of the AhR or Arnt connected to the C-terminus of glutathione S-transferase, GST–AhR (amino acids 1–424) and GST–Arnt (amino acids 88–464), were coexpressed with thioredoxin in *E. coli.* After induction with 20 μM isopropyl-β-D(−)thiogalactopyranoside at 30 °C for 15 h, the chimeric proteins were purified with glutathione-Sepharose affinity column chromatography (greater than 80% purity), treated with thrombin to cut GST off, and used without further purification for gel shift assays. Yeast strain D452-1 (MATa leu2 ura3 his3 trp1) which was generated from D373-4B and D448-2 [28] was transformed with plasmids by the lithium acetate method [29]. Transformed yeast cells were treated with 3 μM β-naphthoflavon for 18 h for induction of β-galactosidase, and expressed β-galactosidase activity was measured as described [28].

Results

Upstream regions responsible for induction by MC

The CAT activity from a chimeric plasmid containing −5.6 kb upstream sequence of the *CYP1A2* gene and the CAT structural gene was induced 3.4-fold by the addition of MC as shown in Fig. 1A. This induction was not found when Hepa-1 and L929 cells were used as host cells (data not shown). These findings agree with the results of similar experiments using the human *CYP1A2* gene [30]. To identify *cis*-acting elements responsible for induction, we constructed a series of deletion plasmids as shown in Fig. 1A. A similar level of induction was observed until deletion from the 5′ end proceeded to −2237, and further deletion to −2063 largely reduced the induced CAT activity. This result shows an important sequence for the induction was localized between −2237 and −2063. We further constructed fine deletion plasmids to delineate the response element as shown in Fig. 1B. Induced CAT activity was gradually reduced with progressive deletion from −2205 to −2120.
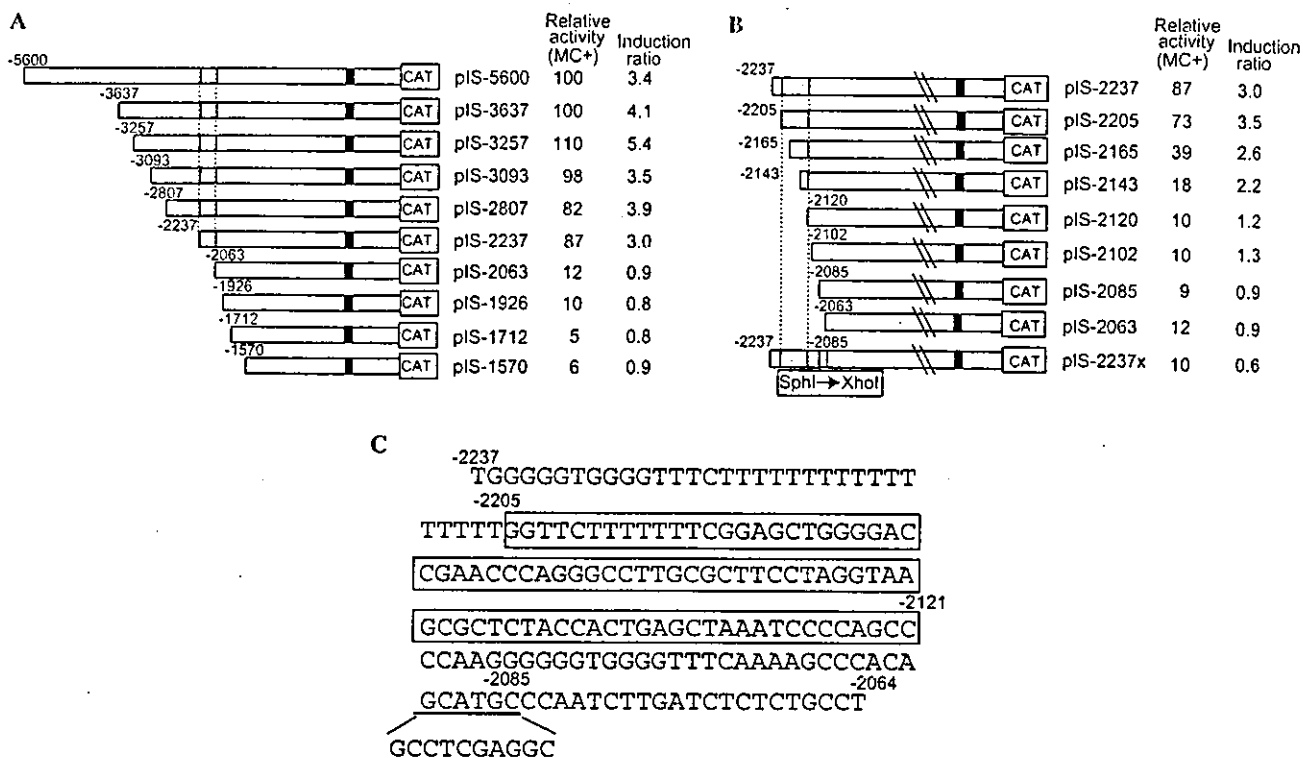
Fig. 1. Schematic representations of *CYP1A2*-CAT chimeric plasmids and their CAT activities in response to MC. (A) DNA fragments from the 5′-upstream region of the *CYP1A2* gene used to construct chimeric plasmids are represented by open bars. The first exon and regions responsible for inducible expression are denoted by filled and shaded boxes, respectively. HepG2 cells were transfected with each of the deletion plasmids (5 µg/plate) and an internal control plasmid (1 µg/plate) with the luciferase gene. Relative CAT activities are presented as percentages of the activity obtained with pIS-5600 in the presence of 1 µM MC. The extent of induction by MC is also shown as the ratio of the induced to the uninduced activity. Values represent means of at least 3 independent determinations. Nucleotide positions of the 5′-flanking sequence are numbered in negative from the start site. (B) Structure of chimeric plasmids with fine deletions and their CAT activities in response to 3-MC. Structure of each deletion plasmid and CAT activity are shown in the same way as in (A). (C) Nucleotide sequence of the regulatory region of transcription in the *CYP1A2* gene. The upstream regulatory region (−2205/−2120) is enclosed by boxes. The *Sph*I site in the downstream region is underlined. Inserted sequence by an *Xho*I linker is shown under the *Sph*I site.

The induction ratio decreased in accordance with the reduction of the induced CAT activity. Insertion of an *Xho*I linker into the *Sph*I site at −2085 completely abolished induced CAT activity, although the construct (pIS-2237x) contained the important region between −2205 and −2120. These results indicate that there are at least two regions responsible for the induction, −2205 to −2120, and a sequence around the *Sph*I site at −2085. The sequence from −2237 to −2064 is shown in Fig. 1C and contains no XRE core sequences (CACGC).

We investigated the transcriptional activity of the sequence (−2237 to −1603) on a heterologous promoter of the *CYP1A1* gene [18] as shown in Fig. 2A. The sequence inserted in the sense orientation showed very weak activity, and this activity was abolished when the sequence from −2237 to −2144 was deleted. On the other hand, a conspicuous induced activity was observed in the reverse orientation when the sequence from −2237 to −2144 was deleted (Fig. 2A). The reason for the orientation-dependent inhibition by the sequence from −2237 to −2144 is not known, and is necessary to be elucidated. Further deletions to −2085 abolished inducible expres-

sion completely. To delineate the 3′ end of the element indispensable for inducible expression, we constructed a series of deletion mutants as shown in Fig. 2B. Even deletions to −2036 (pDR-2036) still possessed inducible CAT activity. We synthesized two oligonucleotides which cover −2097 to −2073 and −2097 to −2079, and separately inserted them into the upstream region of the *CYP1A1* promoter as shown in Fig. 1C. The fragment from −2097 to −2073 gave rise to CAT activity in an MC-dependent and orientation-independent manner, indicating that this 25 bp element is an enhancer. Deletion from −2073 to −2078 completely abolished the activity (B sequence in Fig. 2C).

Involvement of the AhR and Arnt in the inducible expression of the CYP1A2 enhancer

Interestingly, the constructions as shown in Fig. 2C showed inducible expression in Hepa-1 cells as well as HepG2 (Fig. 3). Two Hepa-1-derived cell lines, C4 and C12 cells that are deficient in Arnt and AhR activity [22,23], respectively, were used to examine the
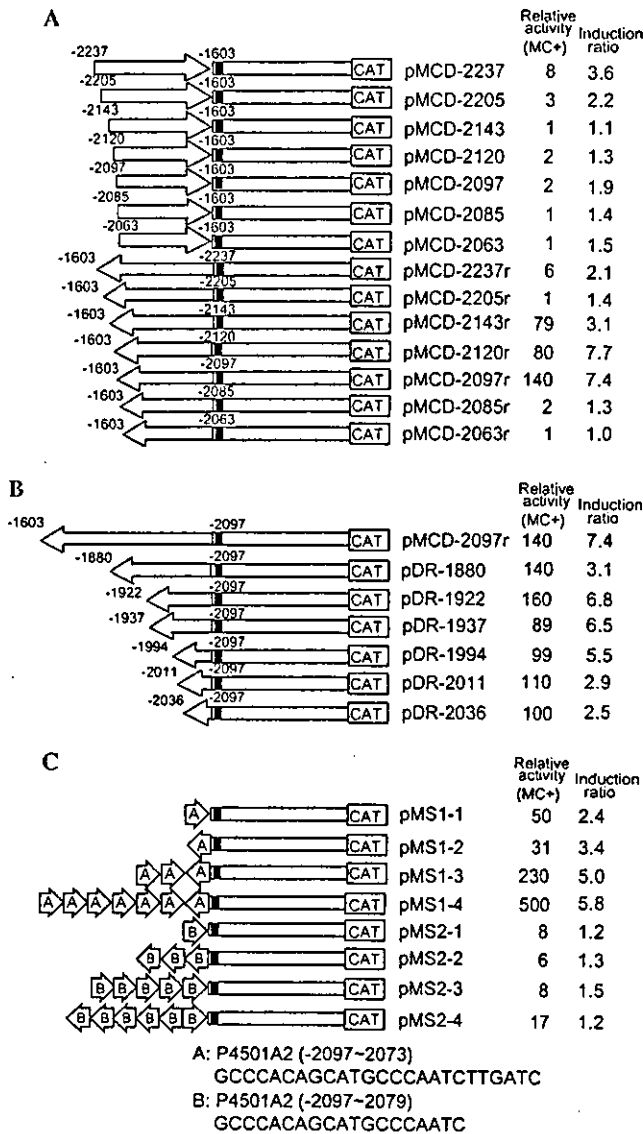
A

	Relative activity (MC+)	Induction ratio
pMCD-2237	8	3.6
pMCD-2205	3	2.2
pMCD-2143	1	1.1
pMCD-2120	2	1.3
pMCD-2097	2	1.9
pMCD-2085	1	1.4
pMCD-2063	1	1.5
pMCD-2237r	6	2.1
pMCD-2205r	1	1.4
pMCD-2143r	79	3.1
pMCD-2120r	80	7.7
pMCD-2097r	140	7.4
pMCD-2085r	2	1.3
pMCD-2063r	1	1.0

B

	Relative activity (MC+)	Induction ratio
pMCD-2097r	140	7.4
pDR-1880	140	3.1
pDR-1922	160	6.8
pDR-1937	89	6.5
pDR-1994	99	5.5
pDR-2011	110	2.9
pDR-2036	100	2.5

C

	Relative activity (MC+)	Induction ratio
pMS1-1	50	2.4
pMS1-2	31	3.4
pMS1-3	230	5.0
pMS1-4	500	5.8
pMS2-1	8	1.2
pMS2-2	6	1.3
pMS2-3	8	1.5
pMS2-4	17	1.2

A: P4501A2 (-2097~2073)
GCCCACAGCATGCCCAATCTTGATC
B: P4501A2 (-2097~2079)
GCCCACAGCATGCCCAATC

Fig. 2. Schematic representation of CYP1A2 enhancer-CAT chimeric plasmids and their CAT activities in response to MC. (A,B) DNA fragments containing the CYP1A2 enhancer were connected in sense or antisense orientation to pMC53c, which contains the CYP1A1 promoter (up to -53 from the transcription-initiation site, see [18]) connected to the CAT structural gene. CAT activity was measured as described in Materials and methods, and normalized by the activity of pMC53c in the presence of MC. Bars show the CYP1A1 sequence. Closed and open boxes show 1st exon and 1st intron, respectively. Arrows indicate length and orientation of DNA fragments of the CYP1A2 gene. Nucleotide positions of the 5'-flanking sequence are numbered in negative from the start site. (C) Synthetic oligonucleotides of the CYP1A2 enhancer were tandemly inserted in the upstream region of the promoter for pMC53c as in A and B. Right arrows represent the natural orientation relative to the transcription; left arrows the inverse orientation. CAT activity is shown in the same way as in A and B. Sequences of the inserted oligonucleotides are shown below.

Fig. 3. Involvement of the AhR and Arnt in the inducible expression of the CYP1A2 enhancer. Inducibility and enhancer activity of the CYP1A2 enhancer and XRE were measured in mutant Hepa-1 cells, C4, and C12 cells. (1) pMC53c, (2) XRE4-pMC53, and (3) pMS1-4. Reaction products of the CAT activity were separated with thin-layer chromatography and a typical autoradiographic result is shown. Cells transfected with the test plasmids were grown in the presence (+) or absence (-) of 1 μM MC.

involvement of the two transcription factors in the activity of the CYP1A2 enhancer. As shown in Fig. 3, inducibility of CAT activity found in the parental cell line was completely abolished in C4 and C12 cells, although some constitutive expression was found particularly in C4 cells.
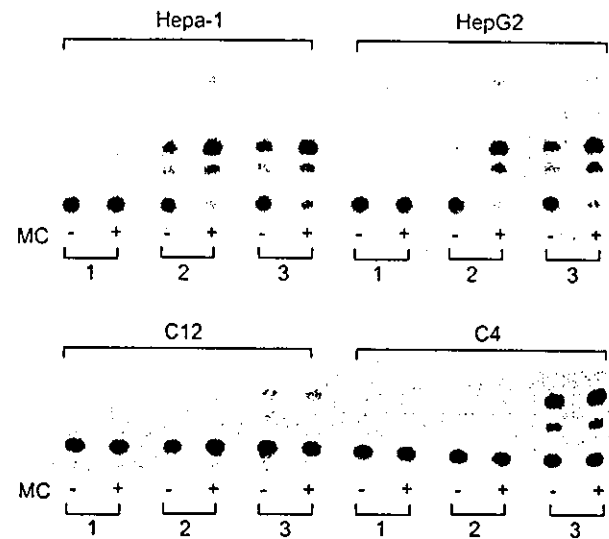
This result shows that both the AhR and Arnt are necessary for inducible expression of the CYP1A2 enhancer.

We used an expression system in yeast to investigate the function of AhR and Arnt in the enhancer activity. As shown in Fig. 4A, a reporter gene containing four tandemly repeated XREs in the promoter region was activated about 20-fold by the addition of β-naphthoflavon as reported previously [31]. However, when a reporter gene containing the CYP1A2 enhancer in the promoter region was used, the resultant β-galactosidase activity was at a similar level to those of negative controls containing no or HRE sequences in the promoter region. Binding activity of the AhR–Arnt heterodimer to the CYP1A2 enhancer was investigated using gel mobility shift assays. Nuclear extracts from HepG2 cells contained an XRE-binding activity derived from the heterodimer only when cells were treated with MC (Fig. 4B) as reported [32]. The band was not effectively diminished by a large excess of unlabeled oligonucleotides carrying the CYP1A2 enhancer (Fig. 4, lanes 8 and 9). Finally, we tested the binding activity of the AhR–Arnt heterodimer to the CYP1A2 enhancer using AhR and Arnt which were bacterially expressed and purified (Fig. 4C). Although the purified proteins were mostly present in aggregate forms (data not shown), the preparation still possessed a strong binding activity to XRE (Fig. 4C, lane 5). On the other hand, no signal was detected when the oligonucleotides for the CYP1A2 enhancer were used as the binding probe (Fig. 4C, lane 1).

Taken together, these results indicate that the AhR–Arnt heterodimer plays an essential role in the inducible
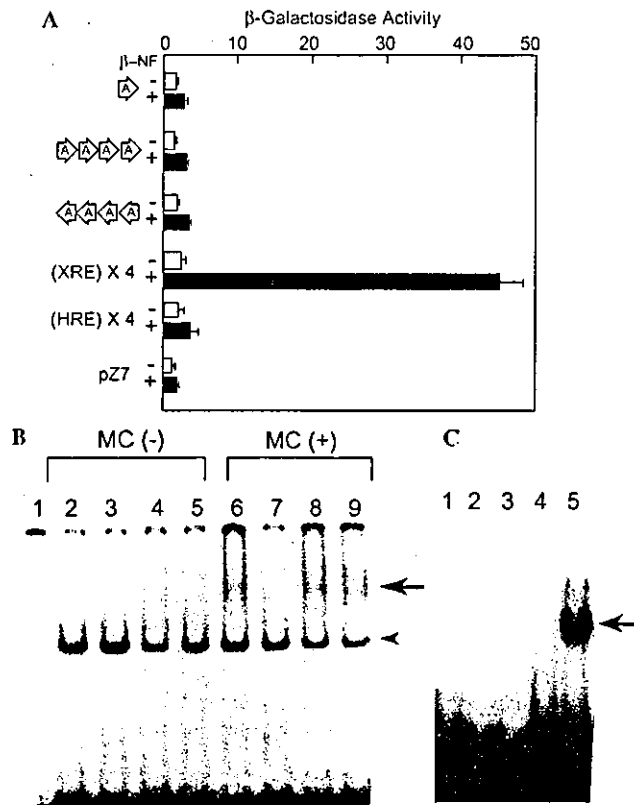
Fig. 4. Lack of binding activity of the AhR–Arnt heterodimer to the CYP1A2 enhancer. (A) Expression of plasmids containing the CYP1A2 enhancer in the yeast which expresses the AhR and Arnt. Arrows show number and orientation of the CYP1A2 enhancer; the sequence is shown in Fig. 2C. Yeast cells were treated with 3 μM β-naphthoflavon at 30 °C for 18 h. β-Galactosidase activity is represented as described [28]. (B) Competition gel mobility shift assay of the CYP1A2 enhancer with XRE using nuclear extracts of HepG2 cells. Labeled XRE sequence (20,000 cpm) was used as a probe. Lane 1, no protein; lanes 2–9, 10 μg of the nuclear extracts on protein base; lanes 3 and 7, 300-fold unlabeled XRE; lanes 4 and 8, 300-fold unlabeled CYP1A2 enhancer (−2205 to −2073); lanes 5 and 9, 300-fold unlabeled CYP1A2 enhancer (−2097 to −2073); lanes 2–5, nuclear extracts of untreated cells; lanes 6–9, nuclear extracts of MC-treated cells. An arrow and arrowhead show positions of specific and nonspecific bands, respectively. (C) Lack of binding activity of the CYP1A2 enhancer to bacterially expressed AhR–Arnt heterodimer. Oligonucleotides for the CYP1A2 enhancer (−2097 to −2073) and two oligonucleotides (−2097 to −2079 and −2087 to −2069) were used for labeled probes in lanes 1, 2, and 3, respectively. XRE was used for probe in lanes 4 and 5 with and without 100-fold excess unlabeled XRE, respectively. An arrow shows the position of the specific band. Incubation of the bacterially expressed AhR or Arnt separately with the XRE probe did not generate any shifted bands (data not shown).

expression of the CYP1A2 enhancer, but that it does not directly bind to the enhancer sequence.

Mutational analysis of the CYP1A2 enhancer

We introduced point mutations systematically into the sequence of the CYP1A2 enhancer in order to identify critical nucleotides for the inducible enhancer activity as shown in Fig. 5. The plasmids with mutations

were transfected into HepG2 cells, and the expressed luciferase activity was measured. Consequently, an imperfect short repeat that mutated in the plasmids E, F, J, and K was found to be important for the inducible expression of the luciferase activity. Furthermore, the nucleotides changed in mutants D and H were found to be necessary for full activity of the enhancer because these mutants showed lower inducibility than the wild type. A notable enhancement in activity was observed in mutants H-1 and I, suggesting the presence of an inhibitory sequence in the enhancer. Additional mutations in the repeated sequence were introduced into mutant G, used as the parental plasmid, which shows higher inducibility than the wild type (Figs. 5A and B). Only a mutation that gave rise to a perfect repeat showed comparable activity with mutant G while the other mutations in the repeated sequence abolished the expression. Six nucleotides of interspace between the units of the repeat were found to be essential for the inducible expression, since the expression was completely abolished by one base pair-deletion or addition (mutants N5 and N7 in Fig. 5B) in the repeated sequence. We searched a database for DNA sequences that contained the repeated sequence separated by 6 base pairs. Interestingly, a DNA sequence which satisfies the requirement was found in the upstream region of the rat CYP1A1 gene (−259 from the transcription-initiation site) [33]. The element of the CYP1A1 gene was found to exhibit an enhancer activity in response to MC as shown in Fig. 5A, although its activity was lower (approximately 60%) than that of the CYP1A2 enhancer.

Binding factor to the CYP1A2 enhancer

Since the AhR–Arnt heterodimer did not directly bind to the CYP1A2 enhancer, we looked for a factor that directly bound to the enhancer in nuclear extracts of HepG2 cells. A specific band was found (Fig. 6A, lane 2), and the intensity and position of the band was not changed by the treatment of cells with MC (data not shown). The band disappeared with a 50-fold excess of unlabeled oligonucleotides of the enhancer (Fig. 6A, lane 3). Similar competition experiments were performed using oligonucleotides, which had the same sequences as those used for construction of mutant plasmids shown in Fig. 5A as competitors. Mutated oligonucleotides with sequences D, E, F, H, J, and K could not compete efficiently with the probe (Fig. 6 upper panel). This result correlated well with the result of the enhancer activity of plasmids with mutated sequences (Fig. 5A). As shown in the lower panel of Fig. 6, the mutated sequences of J and K could not compete with the enhancer even in 400-fold excess. This result suggests that the 3′ unit of the repeat largely contributed to the binding affinity toward the factor. However, oligonucleotides used as binding probes lacking either the

A

Relative Luciferase Activity

	Sequence
1A2	GCCCACAGCATGCCCAATCTTGATC
A	TTCCACAGCATGCCCAATCTTGATC
B	GCTTACAGCATGCCCAATCTTGATC
C	GCCCTTAGCATGCCCAATCTTGATC
D	GCCCACTTCATGCCCAATCTTGATC
E	GCCCACAGTTTGCCCAATCTTGATC
F	GCCCACAGCAATCCCAATCTTGATC
G	GCCCACAGCATGTTCAATCTTGATC
H	GCCCACAGCATGCCTTATCTTGATC
H-I	GCCCACAGCATGCCCTTTCTTGATC
I	GCCCACAGCATGCCCATACTTGATC
J	GCCCACAGCATGCCCAATTATGATC
K	GCCCACAGCATGCCCAATCTATATC
L	GCCCACAGCATGCCCAATCTTGTAC
XRE x 4	
pGL3pro	
1A1	GTGCTGTCCATGGAGCGCCTTGAAA

B

Relative Luciferase Activity

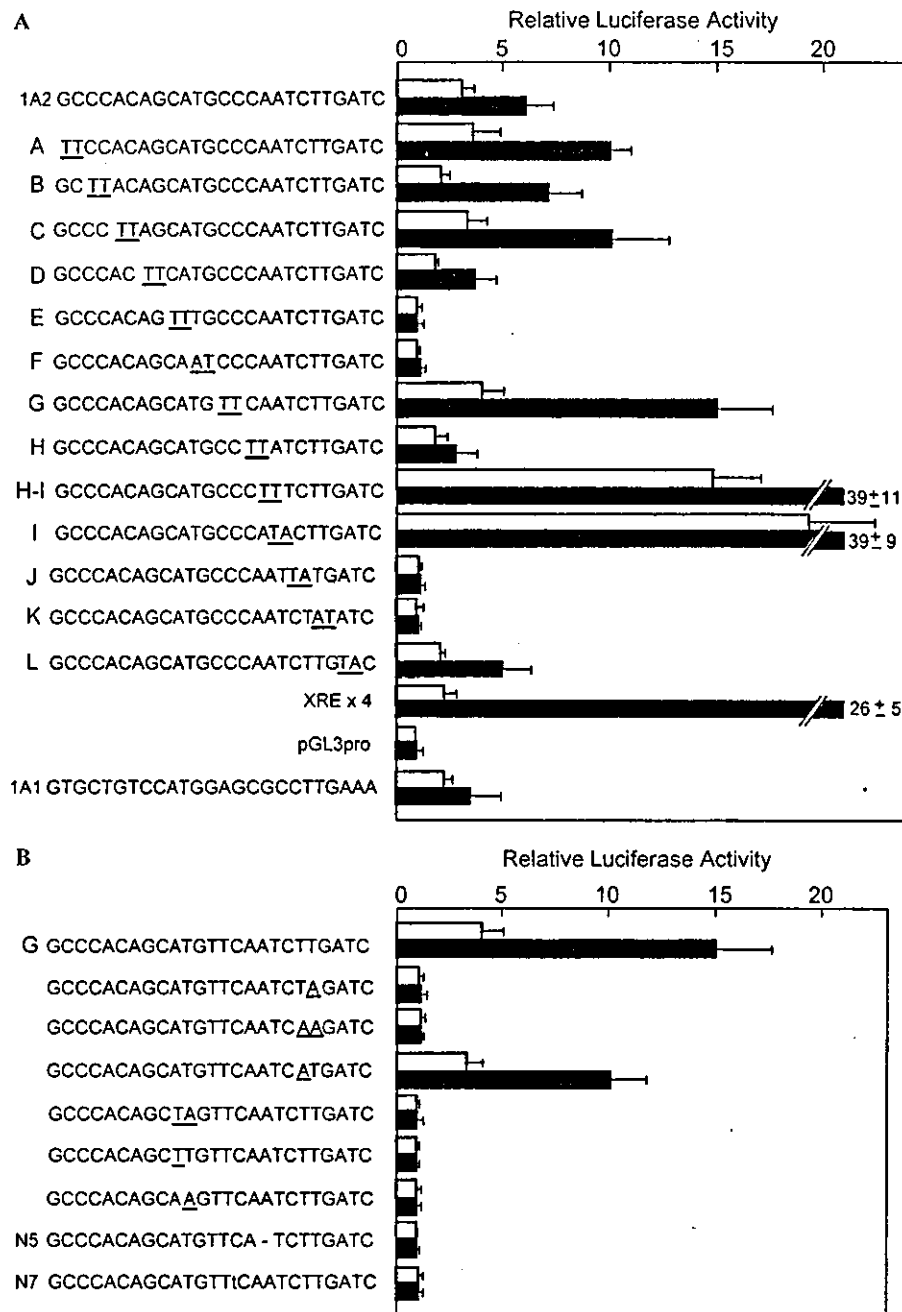|	Sequence
G	GCCCACAGCATGTTCAATCTTGATC
	GCCCACAGCATGTTCAATCTAGATC
	GCCCACAGCATGTTCAATCAAGATC
	GCCCACAGCATGTTCAATCATGATC
	GCCCACAGCTAGTTCAATCTTGATC
	GCCCACAGCTTGTTCAATCTTGATC
	GCCCACAGCAAGTTCAATCTTGATC
N5	GCCCACAGCATGTTCA-TCTTGATC
N7	GCCCACAGCATGTTtCAATCTTGATC

Fig. 5. Mutational analysis of the *CYP1A2* enhancer. (A) Effect of mutations in the *CYP1A2* enhancer on the transcriptional activity. Reporter plasmids (2 μg) containing two copies of the mutated sequences inserted upstream of the promoter region of pGL3pro were cotransfected with the internal control plasmid (3 μg) of lacZ, and the expressed luciferase activity was measured. Cells transfected with the test plasmids were grown in the presence (filled bars) or absence (open bars) of 1 μM MC for 40 h. Nucleotides different from the wild type *CYP1A2* enhancer are underlined. The uninduced luciferase activity of pGL3pro is used as a unit. (B) Mutational analysis of direct repeat in the *CYP1A2* enhancer. Mutated nucleotides are underlined. A deletion in N5 is denoted by a dash. An insertion of T in N7 is indicated with a small letter.

5′ or 3′ repeated sequence could not bind to the factor (data not shown).

Association of the binding factor with the AhR–Arnt heterodimer

To examine the interaction between the AhR–Arnt heterodimer and the factor binding to the *CYP1A2* en-

hancer, bacterially expressed AhR–Arnt was mixed with nuclear extracts of HepG2 cells, and the mixture was then used for gel mobility shift assays. As shown in Fig. 7A, addition of the AhR–Arnt resulted in decreased intensity of the band specifically bound to the enhancer. On the other hand, the intensity of bands of the GC box sequence bound by Sp1 was not affected by the AhR–Arnt complex, as shown in Fig. 7C, although Sp1 is

synergistic activation by simultaneous expression of the two factors was not clearly observed (Fig. 8). To ex- amine whether or not the DNA-binding capacity of the factors is necessary for the transactivation activity, we constructed a plasmid with a mutation, AGA for Arg39 to ATA for Ile in the basic sequence of the AhR, and cotransfected it with a reporter plasmid containing XRE

AHR-Arnt

1 2 3 4 5 6 7

A

AhR
Arnt

1 2 3 4

B

AHR-Arnt

1 2 3 4 5 6 7

C

Fig. 7. Interaction of the binding factor to the CYP1A2 enhancer with the AhR–Arnt complex. (A) Interaction of the enhancer-binding factor with AhR–Arnt. Nuclear extracts from HepG2 cells were mixed with increasing amounts of bacterially expressed AhR and Arnt, and ana- lyzed by gel shift assays using the oligonucleotides of the CYP1A2 enhancer as a labeled probe. Lane 1, no protein; lanes 2–7, 5 μg of the nuclear extracts on protein base; lanes 3–7, 0.15, 0.3, 0.45, 0.6, and 0.75 μg each of AhR and Arnt, respectively. An arrow shows the po- sition of the specific band. (B) Association of the binding factor with Arnt or AhR. Bacterially expressed AhR or Arnt was separately in- cubated with HepG2 nuclear extracts and analyzed by gel mobility shift assays. Lane 1, no protein; lanes 2–4, 5 μg of protein; lanes 3 and 4, AhR and Arnt, respectively. (C) Interaction of Sp1 with AhR and Arnt. The oligonucleotide for BTE (a GC box, see [39]) was used as a probe. Experiments were done in a similar way to those in (A). The arrow shows the position of the specific band of Sp1 and BTE.

We examined transactivation activity of the AhR and Arnt for the CYP1A2 enhancer and XRE in HepG2 cells. The luciferase activity of the reporter plasmid containing the CYP1A2 enhancer or XRE was enhanced by the coexpression of the AhR or Arnt, although

Activation of the CYP1A2 enhancer with coexpression of the Arnt, AhR, and AhR mutant

reported to possess some affinity to the AhR and Arnt [34]. This result may be explained by assuming that a fairly strong interaction occurs between the AhR–Arnt complex and the enhancer-binding factor, and that this interaction prevents the factor from migrating into ac- rylamide gels because almost all of the AhR–Arnt com- plex was present as aggregates which could not migrate into gels. We separately incubated the AhR or Arnt with the nuclear extracts and used them for gel shift assays. As shown in Fig. 7B, Arnt trapped the enhancer-binding factor, indicating that the AhR–Arnt heterodimer inter- acts with the factor through the Arnt protein.

Competitor (X400)

- B C D E F G H I J K L
1A2

1 2 3 4 5 6 7 8 9 10 11 12 13 14

Competitor (X50)

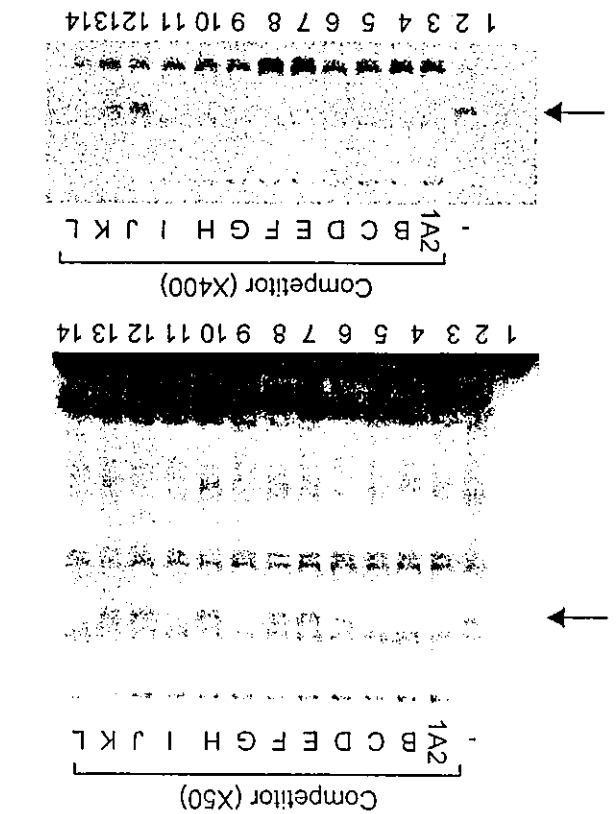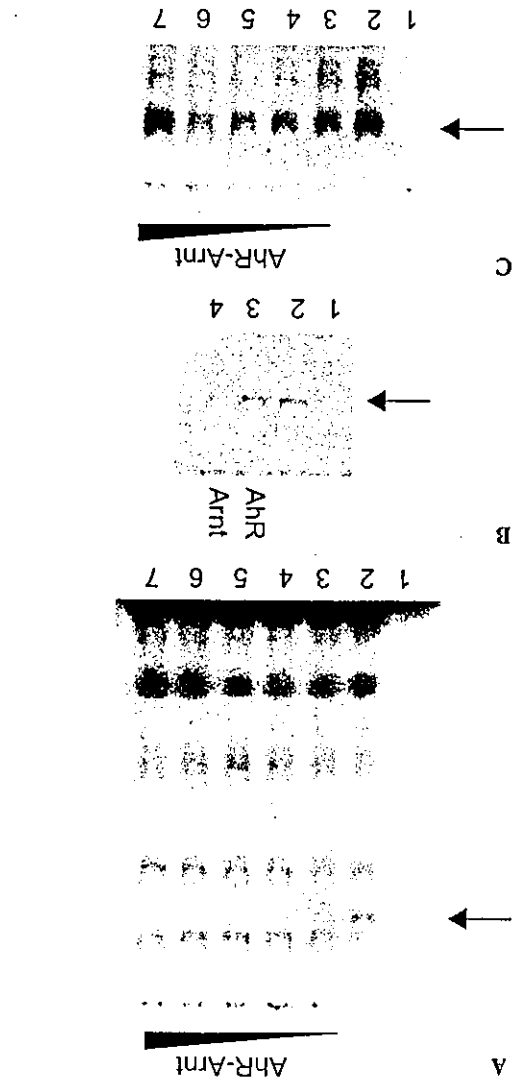- B C D E F G H I J K L
1A2

1 2 3 4 5 6 7 8 9 10 11 12 13 14

Fig. 6. Analysis of binding factors to the CYP1A2 enhancer. Nuclear extracts of HepG2 cells treated with MC for 2h were analyzed using oligonucleotides for the CYP1A2 enhancer as a probe in the gel shift assay. An arrow shows the position of the specific band. Lane 1, no protein; lanes 2–14, 5 μg of the nuclear extracts on protein base; lanes 3–14, wild type competitor and mutated competitors B–L have the same sequences as those (mut B–L) shown in Fig. 5A, respectively. Fifty and 400-fold excess of competitors was used in the gel mobility shift assay on upper and lower panels, respectively.

A

CYP1A2 enhancer

Relative Luciferase Activity

MC	– +	– +	– +	– +	– +	– +
AhR	– –	+ +	– –	– –	+ +	– –
AhR(Arg39Ile)	– –	– –	+ +	– –	– –	+ +
Arnt	– –	– –	– –	+ +	+ +	+ +
1A2 enh x 4	+ +	+ +	+ +	+ +	+ +	+ +

B

XRE

Relative Luciferase Activity

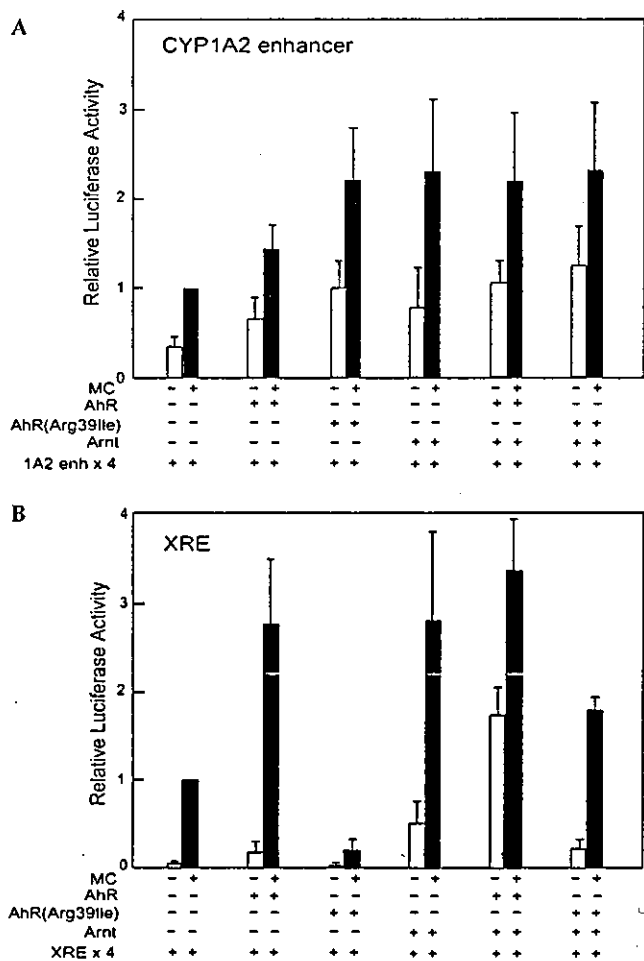| MC	– +	– +	– +	– +	– +	– +
AhR	– –	+ +	– –	– –	+ +	– –
AhR(Arg39Ile)	– –	– –	+ +	– –	– –	+ +
Arnt	– –	– –	– –	+ +	+ +	+ +
XRE x 4	+ +	+ +	+ +	+ +	+ +	+ +

Fig. 8. Activation of the *CYP1A2* enhancer activity by transfection with AhR and Arnt expression plasmids. Reporter plasmids (1 μg) containing four copies of *CYP1A2* enhancer (A) and XRE (B) in the promoter region were transfected into HepG2 cells with various combinations of expression plasmids (1 μg each) for Arnt, AhR, and a dominant negative mutant (AhR Arg39Ile) of the AhR with a missense mutation in the basic sequence. The internal control plasmid (2 μg) of lacZ for efficiency of transfection was used, and total DNA was adjusted to 5 μg by adding the pEFBOS vector plasmid. The luciferase activity induced by the addition of MC from cells transfected with the only reporter plasmid is used as a unit. Cells transfected with plasmids were grown in the presence (+) or absence (–) of 1 μM MC for 40 h.

or *CYP1A2* enhancer sequences. As expected, the mutated AhR repressed 5.0-fold the luciferase activity of the reporter plasmid containing XRE sequences as shown in Fig. 8B. In contrast, the dominant negative mutant of the AhR activated the luciferase activity Fig. 8A more strongly than the wild type AhR, when the reporter plasmid containing *CYP1A2* enhancer sequences was used. This result clearly demonstrates that the DNA-binding activity of the AhR is not necessary for the transcriptional activation of the *CYP1A2* enhancer. In the yeast expression system used in Fig. 4, the mutant of the AhR induced no β-galactosidase activity of the reporter plasmid containing XRE sequences when it was coexpressed with Arnt (data not shown).

Discussion

We have identified two regions responsible for inducible expression of the rat *CYP1A2* gene by MC. The upstream one localized between −2205 and −2120 may function as a region that enhances the activity of the downstream enhancer. Tandem repeats of the sequence on a heterologous promoter did not exhibit any transcriptional activity (data not shown). The downstream one which consists of 25 base pairs showed an enhancer activity dependent on inducers such as MC, although the activity was not detected in the context of the *CYP1A2* promoter without the upstream region. A mutational analysis disclosed that two short repeated sequences in the enhancer sequence are important for enhancer activity. This feature of the *CYP1A2* enhancer is not shared with the classical XRE found in various MC-inducible genes; it contains an invariant core sequence, CACGC, which is recognized and bound by the AhR–Arnt heterodimer [14,15]. It is clear that the AhR–Arnt heterodimer could not directly bind to the *CYP1A2* enhancer, therefore suggesting the presence of a mediator between the DNA sequence and the AhR–Arnt heterodimer (Figs. 4 and 7). Finding that a dominant negative mutant of the AhR with a mutation in the basic region activates the *CYP1A2* enhancer but not XRE supports the indirect interaction between the AhR and the *CYP1A2* enhancer. We would like to propose that this novel type of XRE be called XRE II to distinguish it from the classical XRE. Database search for the enhancer sequence revealed that several genes contain this type of XRE (data not shown). It is interesting to note that the rat *CYP1A1* gene also contains XRE II. Functional analysis of the sequence revealed that it possesses an enhancer activity which responds to MC (Fig. 5A). Cooperation of both types of XRE is possibly involved in the inducible expression of the gene. This finding strongly suggests that XRE II is widely distributed in various promoters of MC-inducible genes.

The indirect binding of the AhR and Arnt heterodimer to the *CYP1A2* enhancer is reminiscent of coactivators such as CBP and p300 in the transcriptional mechanism [35]. Several PAS domain-containing proteins such as SRC1 and TIF2 are known to function as coactivators that act as bridges between enhancer-binding factors and general transcription factors in transcription activation [36,37]. Our results demonstrate that the AhR–Arnt complex does not only work as a sequence-specific transcription factor which directly binds to the classical XRE but could also act as a coactivator in the transcription via XRE II. These different transcription mechanisms mediated by the AhR–Arnt heterodimer are schematically depicted in Fig. 9. For detailed analysis of this transcription mechanism through the *CYP1A2* enhancer, isolation and characterization of the sequence-specific transcription factor
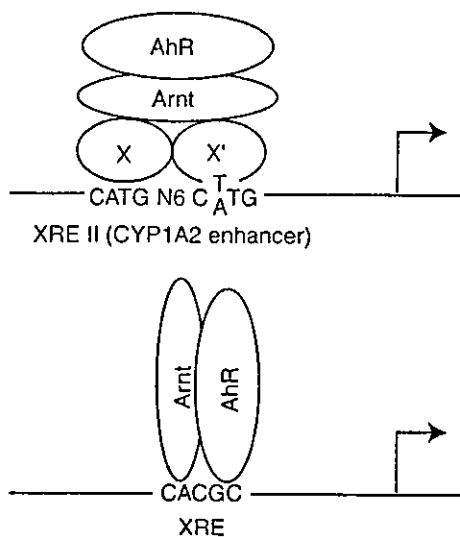
Fig. 9. Schematic representation of two types of transcription mechanisms mediated by the AhR–Arnt heterodimer. Upper, the AhR–Arnt heterodimer functions as a coactivator in the rat *CYP1A2* gene. X and X' denote subunits of the binding factor to XRE II or *CYP1A2* enhancer. The dimeric structure of the binding factor is hypothetical. Lower, the classical model of induction of genes mediated by AhR–Arnt heterodimer. The AhR–Arnt heterodimer functions as the transcription factor that directly binds to XRE.

which directly bind to the *CYP1A2* enhancer are necessary, and studies along this line are now in progress.

It is reported that two regions (−2532 to −2423 and −2195 to −1987) in the human *CYP1A2* gene are involved in the inducible expression by MC. The upstream region contained an XRE sequence (termed X1) and no XREs were present in the downstream region although an analogous sequence (termed X2) to XRE is present [38]. Furthermore, several *cis*-acting elements such as AP-1-binding site, CAT box, HNF-1-binding site, and TATA box are reported to be present [38]. In the regions, no typical XRE II sequences were found, suggesting that different induction mechanism is present between the rat and human genes. However, it is also possible in the human gene that XRE II with a sequence deviated from that of typical XRE II may be present and activate the transcription by the aid of the reported DNA elements nearby localized.

Isosafrole did not induce the expression of reporter genes driven by the *CYP1A2* enhancer (data not shown), suggesting that the *cis*-acting element responsible for the induction by isosafrole and related CYP1A2-specific inducers is carried by other regions of the *CYP1A2* gene.

Acknowledgments

References

[1] D.R. Nelson, L. Koymans, T. Kamataki, J.J. Stegeman, R. Feyereisen, D.J. Waxman, M.R. Waterman, O. Gotoh, M.J. Coon, R.W. Estabrook, I.C. Gunsalus, D.W. Nebert, P450 superfamily: update on new sequences, gene mapping, accession numbers and nomenclature, Pharmacogenetics 6 (1996) 1–42.

[2] A.R. Boobis, A.M. Lynch, S. Murray, R. de la Torre, A. Solans, M. Farre, J. Segura, N.J. Gooderham, D.S. Davies, CYP1A2-catalyzed conversion of dietary heterocyclic amines to their proximate carcinogens is their major route of metabolism in humans, Cancer Res. 54 (1994) 89–94.

[3] J.A. Goldstein, P. Linko, Differential induction of two 2,3,7,8-tetrachlorodibenzo-p-dioxin-inducible forms of cytochrome P-450 in extrahepatic versus hepatic tissues, Mol. Pharmacol. 25 (1984) 185–191.

[4] C. Wei, R.J. Caccavale, J.J. Kehoe, P.E. Thomas, M.M. Iba, CYP1A2 is expressed along with CYP1A1 in the human lung, Cancer Lett. 171 (2001) 113–120.

[5] M. Lechevrel, A.G. Casson, C.R. Wolf, L.J. Hardie, M.B. Flinterman, R. Montesano, C.P. Wild, Characterization of cytochrome P450 expression in human oesophageal mucosa, Carcinogenesis 20 (1999) 243–248.

[6] D.C. Morse, A.P. Stein, P.E. Thomas, H.E. Lowndes, Distribution and induction of cytochrome P450 1A1 and 1A2 in rat brain, Toxicol. Appl. Pharmacol. 152 (1998) 232–239.

[7] O. Hankinson, The aryl hydrocarbon receptor complex, Annu. Rev. Pharmacol. Toxicol. 35 (1995) 307–340.

[8] K. Sogawa, Y. Fujii-Kuriyama, Ah receptor, a novel ligand-activated transcription factor, J. Biochem. 122 (1997) 1075–1079.

[9] K. Kawajiri, O. Gotoh, Y. Tagashira, K. Sogawa, Y. Fujii-Kuriyama, Titration of mRNAs for cytochrome P-450c and P-450d under drug-inductive conditions in rat livers by their specific probes of cloned DNAs, J. Biol. Chem. 259 (1984) 10145–10149.

[10] S. Kimura, F.J. Gonzalez, D.W. Nebert, Tissue-specific expression of the mouse dioxin-inducible P₁450 and P₃450 genes: differential transcriptional activation and mRNA stability in liver and extrahepatic tissues, Mol. Cell. Biol. 6 (1986) 1471–1477.

[11] D.S. Pasko, K.W. Boyum, S.N. Merchant, S.C. Chalberg, J.B. Fagan, Transcriptional and post-transcriptional regulation of the genes encoding cytochromes P-450c and P-450d in vivo and in primary hepatocyte cultures, J. Biol. Chem. 263 (1988) 8671–8676.

[12] J.V. Schmidt, G.H.-T. Su, J.K. Reddy, M.C. Simon, C.A. Bradfield, Characterization of a murine Ahr null allele: involvement of the Ah receptor in hepatic growth and development, Proc. Natl. Acad. Sci. USA 93 (1996) 6731–6736.

[13] J. Mimura, K. Yamashita, K. Nakamura, M. Morita, T.N. Takagi, K. Nakao, M. Ema, K. Sogawa, M. Yasuda, M. Katsuki, Y. Fujii-Kuriyama, Loss of teratogenic response to 2,3,7,8-tetrachlorodibenzo-p-dioxin (TCDD) in mice lacking the Ah (dioxin) receptor, Genes Cells 2 (1997) 645–654.

[14] K. Sogawa, R. Nakano, A. Kobayashi, Y. Kikuchi, N. Ohe, N. Matsushita, Y. Fujii-Kuriyama, Possible function of Ah receptor nuclear translocator (Arnt) homodimer in transcriptional regulation, Proc. Natl. Acad. Sci. USA 92 (1995) 1936–1940.

[15] S.G. Bacsi, S. Reisz-Porszasz, O. Hankinson, Orientation of the heterodimeric aryl hydrocarbon (dioxin) receptor complex on its asymmetric DNA recognition sequence, Mol. Pharmcol. 47 (1995) 432–438.

[16] A. Fujisawa-Sehara, K. Sogawa, M. Yamane, Y. Fujii-Kuriyama, Characterization of xenobiotic responsive elements upstream from the drug-metabolizing cytochrome P-450c gene: a similarity to glucocorticoid regulatory elements, Nucleic Acids Res. 15 (1987) 4179–4191.

[17] K. Sogawa, O. Gotoh, K. Kawajiri, T. Harada, Y. Fujii-Kuriyama, Complete nucleotide sequence of a methylcholan-

threne-inducible cytochrome P-450 (P-450d) gene in the rat, J. Biol. Chem. 260 (1985) 5026-5032.

[18] A. Yanagida, K. Sogawa, K.-I. Yasumoto, Y. Fujii-Kuriyama, A novel *cis*-acting DNA element required for a high level of inducible expression of the rat P-450c gene, Mol. Cell. Biol. 10 (1990) 1470-1475.

[19] S. Mizushima, S. Nagata, pEF-BOS, a powerful mammalian expression vector, Nucleic Acids Res. 18 (1990) 5322.

[20] G.L. Semenza, G.L. Wang, A nuclear factor induced by hypoxia via de novo protein synthesis binds to the human erythropoietin gene enhancer at a site required for transcriptional activation, Mol. Cell. Biol. 12 (1992) 5447-5454.

[21] J. Nikawa, K. Hosaka, S. Yamashita, Differential regulation of two myo-inositol transporter genes of *Saccharomyces cerevisiae*, Mol. Microbiol. 10 (1993) 955-961.

[22] O. Hankinson, Single-step selection of clones of a mouse hepatoma line deficient in aryl hydrocarbon hydroxylase, Proc. Natl. Acad. Sci. USA 76 (1979) 373-376.

[23] C. Legraverend, R.R. Hannah, H.J. Eisen, I.S. Owens, D.W. Nebert, O. Hankinson, Regulatory gene product of the Ah locus. Characterization of receptor mutants among mouse hepatoma clones. J. Biol. Chem. 257 (1982) 6402-6407.

[24] A. Fujisawa-Sehara, K. Sogawa, C. Nishi, Y. Fujii-Kuriyama, Regulatory DNA elements localized remotely upstream from the drug-metabolizing cytochrome P-450c gene, Nucleic Acids Res. 14 (1986) 1465-1477.

[25] C.M. Gorman, L.F. Moffat, B.H. Howard, Recombinant genomes which express chloramphenicol acetyltransferase in mammalian cells, Mol. Cell. Biol. 2 (1982) 1044-1051.

[26] J.D. Dignam, R.M. Lebovitz, R.G. Roeder, Accurate transcription initiation by RNA polymerase II in a soluble extract from isolated mammalian nuclei, Nucleic Acids Res. 11 (1983) 1475-1489.

[27] A. Fujisawa-Sehara, M. Yamane, Y. Fujii-Kuriyama, A DNA-binding factor specific for xenobiotic responsive elements of P-450c gene exists as a cryptic form in cytoplasm: its possible translocation to nucleus, Proc. Natl. Acad. Sci. USA 85 (1988) 5859-5863.

[28] K. Hosaka, T. Murakami, T. Kodaki, J. Nikawa, S. Yamashita, Repression of choline kinase by inositol and choline in *Saccharomyces cerevisiae*, J. Bacteriol. 172 (1990) 2005-2012.

[29] H. Ito, Y. Fukuda, K. Murata, A. Kimura, Transformation of intact yeast cells treated with alkali cations, J. Bacteriol. 153 (1983) 163-168.

[30] L.C. Quattrochi, R.H. Tukey, The human cytochrome *Cyp1A2* gene contains regulatory elements responsive to 3-methylcholanthrene, Mol. Pharmacol. 36 (1989) 66-71.

[31] L.A. Carver, V. Jackiw, C.A. Bradfield, The 90-kDa heat shock protein is essential for Ah receptor signaling in a yeast expression system, J. Biol. Chem. 269 (1994) 30109-30112.

[32] N. Matsushita, K. Sogawa, M. Ema, A. Yoshida, Y. Fujii-Kuriyama, A factor binding to the xenobiotic responsive element (XRE) of P-4501A1 gene consists of at least two helix–loop–helix proteins, Ah receptor and Arnt, J. Biol. Chem. 268 (1993) 21002-21006.

[33] K. Sogawa, O. Gotoh, K. Kawajiri, Y. Fujii-Kuriyama, Distinct organization of methylcholanthrene- and phenobarbital-inducible cytochrome P-450 genes in the rat, Proc. Natl. Acad. Sci. USA 81 (1984) 5066-5070.

[34] A. Kobayashi, K. Sogawa, Y. Fujii-Kuriyama, Cooperative interaction between AhR–Arnt and Sp1 for the drug-inducible expression of CYP1A1 gene, J. Biol. Chem. 271 (1996) 12310-12316.

[35] J.C. Chrivia, R.P.S. Kwok, N. Lamb, M. Hagiwara, M.R. Montminy, R.H. Goodman, Phosphorylated CREB binds specifically to the nuclear protein CBP, Nature 365 (1993) 855-859.

[36] T.P. Yao, G. Ku, N. Zhou, R. Scully, D.M. Livingston, The nuclear hormone receptor coactivator SRC-1 is a specific target of p300, Proc. Natl. Acad. Sci. USA 93 (1996) 10626-10631.

[37] J.J. Voegel, M.J.S. Heine, C. Zechel, P. Chambon, H. Gronemeyer, TIF2, a 160 kDa transcriptional mediator for the ligand-dependent activation function AF-2 of nuclear receptors, EMBO J. 15 (1996) 3667-3675.

[38] L.C. Quattrochi, T. Vu, R.H. Tukey, The human CYP1A2 gene and induction by 3-methylcholanthrene. A region of DNA that supports AH-receptor binding and promoter-specific induction, J. Biol. Chem. 269 (1994) 6949-6954.

[39] H. Imataka, K. Sogawa, K.-I. Yasumoto, Y. Kikuchi, K. Susano, A. Kobayashi, M. Hayami, Y. Fujii-Kuriyama, Two regulatory proteins that bind to the basic transcription element (BTE) a GC box sequence in the promoter region of the rat P-4501A1 gene, EMBO J. 11 (1992) 2671-3663.

HLF/HIF-2α is a key factor in retinopathy of prematurity in association with erythropoietin

Masanobu Morita[1], Osamu Ohneda[2],
Toshiharu Yamashita[1,2], Satoru Takahashi[2],
Norio Suzuki[2], Osamu Nakajima[2],
Shimako Kawauchi[2], Masatsugu Ema[1],
Shigeki Shibahara[3], Tetsuo Udono[4],
Koji Tomita[4], Makoto Tamai[4],
Kazuhiro Sogawa[1], Masayuki Yamamoto[2]
and Yoshiaki Fujii-Kuriyama[1,2,5]

[1]Department of Chemistry, Graduate School of Science, Tohoku
University, Aoba, Aoba-ku, Sendai, 980-8578, [2]Center for Tsukuba
Advanced Research Alliance and Institute of Basic Medical Sciences,
University of Tsukuba, Tennoudai 1-1-1, Tsukuba, 305-8577,
[3]Department of Molecular Biology and Applied Physiology and
[4]Department of Ophthalmology, Tohoku University School of
Medicine, 2-1 Seiryo-cho, Aoba-ku, Sendai, 980-8575, Japan

[5]Corresponding author
e-mail: ykfujii@tara.tsukuba.ac.jp

M.Morita and O.Ohneda contributed equally to this work

An HLF (HIF-1α-like factor)/HIF-2α-knockout mouse
is embryonic lethal, preventing investigation of HLF
function in adult mice. To investigate the role of
HLF in adult pathological angiogenesis, we generated
HLF-knockdown ($HLF^{kd/kd}$) mice by inserting a neo-
mycin gene sandwiched between two loxP sequences
into exon 1 of the HLF gene. $HLF^{kd/kd}$ mice expressing
80–20% reduction, depending on the tissue, in wild-
type HLF mRNA were fertile and apparently normal.
Hyperoxia–normoxia treatment, used as a murine
model of retinopathy of prematurity (ROP), induced
neovascularization in wild-type mice, but not in
$HLF^{kd/kd}$ mice, whereas prolonged normoxia following
hyperoxic treatment caused degeneration of retinal
neural layers in $HLF^{kd/kd}$ mice due to poor vasculari-
zation. Cre-mediated removal of the inserted gene
recovered normal HLF expression and retinal neovas-
cularization in $HLF^{kd/kd}$ mice. Expression levels of
various angiogenic factors revealed that only erythro-
poietin (Epo) gene expression was significantly
affected, in parallel with HLF expression. Together
with the results from intraperitoneal injection of Epo
into $HLF^{kd/kd}$ mouse, this suggests that Epo is one of
the target genes of HLF responsible for experimental
ROP.
Keywords: erythropoietin/HLF/neovascularization/
retinopathy/VEGF

Introduction

Retinal neovascularization is the most common cause of
retinopathy of prematurity (ROP), diabetic retinopathy and
age-related macular degeneration, which eventually leads
to visual loss (Prost, 1988; Moss et al., 1994). Numerous
clinical and experimental observations have indicated that
ischemia or hypoxia triggers retinal neovascularization
through an excessive production of one or more angio-
genic factors. Identification of these factors is an important
step toward understanding the mechanism of pathological
angiogenesis and development of specific treatments for
diseases involving angiogenesis, such as proliferative
retinopathy, tumor growth and atherosclerosis. Among
multiple factors known to be responsible for retinal
neovascularization, many groups have reported vascular
endothelial growth factor (VEGF) to be important (Aiello
et al., 1995; Alon et al., 1995; Pierce et al., 1995; Seo et al.,
1999). These groups have shown that VEGF is upregulated
in a mouse model of retinal neovascularization (Pierce
et al., 1995) and that overexpression of VEGF in
transgenic mice stimulates retinal neovascularization
(Okamoto et al., 1997; Tobe et al., 1998). They have
also shown that VEGF antagonists or kinase inhibitors of
the VEGF receptor prevent retinal neovascularization
(Aiello et al., 1995; Seo et al., 1999).

The transcription factors HIF-1α (hypoxia-inducible
factor-1α) (Wang et al., 1995) and HLF (Ema et al., 1997)
[HIF-1α-like factor, also known as EPAS1 (Tian et al.,
1997) and HIF-2α (Wenger and Gassmann, 1997)] play
important roles in embryonic vascularization, and HIF-1α
and HLF also activate the expression of genes such as
VEGF (Liu et al., 1995; Forsythe et al., 1996),
erythropoietin (Epo) (Wang and Semenza, 1993) and a
series of glycolytic enzymes (Firth et al., 1994) in response
to ischemic or hypoxic conditions. The two factors are
substantially similar in their primary structures and
belong to a growing superfamily of transcription factors
characterized by structural motifs such as basic helix–
loop–helix and PAS (a conserved sequence among Per,
Arnt and Sim) domains. Under normoxic conditions,
HIF-1α is negatively regulated by ubiquitylation and
proteasomal degradation (Kallio et al., 1999). Prolyl
hydroxylation is required for the interaction between
HIF-1α and von Hippel-Lindau (VHL) protein, which
plays a critical role in the ubiquitylation of HIF-1α
(Epstein et al., 2001). When the oxygen concentration is
reduced, these transcription factors are stabilized and form
a heterodimer with another bHLH/PAS protein, Arnt. The
heterodimer activates genes encoding angiogenic and
hematopoietic factors by binding to the hypoxia respon-
sive element (HRE) in their promoter (Semenza and
Wang, 1992; Wang et al., 1995; Ema et al., 1997; Wenger
and Gassmann, 1997). However, the modes of expression
of HLF and HIF-1α differ substantially in various tissues
of adult mice and during developmental processes (Ema
et al., 1997; Jain et al., 1998), indicating that they have
their own specific physiological functions *in vivo*.

Gene targeting technology has been utilized to investigate the function of HLF and HIF-1α, and has revealed that their complete deficiency results in developmental arrest and embryonic lethality. Histopathological analyses of homozygotic mutant embryos showed that HLF deficiency either causes severe vascular defects in both the yolk sac and embryo proper (Peng *et al.*, 2000) or displays pronounced bradycardia due to defective catecholamine production (Tian *et al.*, 1998). In contrast, HIF-1α-deficient mice manifested neural tube defects and cardiovascular malformations (Iyer *et al.*, 1998; Ryan *et al.*, 1998). Although the functions of these two transcription factors appear distinct, embryonic lethality prevented a detailed analysis of their contribution to angiogenesis in adult animals.

In this study, we generated *HLF* knockdown mice by inserting a neomycin resistance gene, sandwiched between two loxP sequences, into exon 1 of the *HLF* gene that encodes the untranslated region (5′-UTR) of HLF mRNA. In these mice, HLF mRNA was expressed at a much lower level by leaky transcription through a double poly(A) signal of the *neo* gene. These mice are viable and fertile without any evident pathological abnormality. Using these mutant mice, we report the essential roles of HLF in the mouse model of ROP by regulating the expression of the Epo gene.

Results

Targeting of the HLF gene by homologous recombination

To investigate the role of HLF in mice, a targeting vector was designed so that the mouse *HLF* gene may be disrupted by inserting a PGK promoter–neomycin gene cassette, which is sandwiched between two loxP sequences, into exon 1 that encodes the 5′-UTR sequence by homologous recombination (Figure 1A). If the double poly(A) signal downstream of the *neo* gene does not work completely, the mRNA encoding HLF in the sequence continuing from the *neo* sequence can be produced because of leaky transcription through the double poly(A) signal at the end of the *neo* gene. The embryonic stem (ES) cell line (clone 144) heterozygous for the recombinant allele (*HLF*$^{kd/+}$) was established by positive–negative selection (Figure 1B) and used to generate chimeric mice by blastocyst injection. Resulting chimeric mice were crossed with wild-type C57BL/6J mice to obtain mice heterozygous for the mutated *HLF* gene (*HLF*$^{kd/+}$).

Mice heterozygous for the *HLF*^{kd} gene were phenotypically indistinguishable from their wild-type littermates and were interbred to yield mice homozygous for the mutated allele (*HLF*$^{kd/kd}$). Genotyping of the newborn mice revealed that the *HLF*$^{kd/kd}$ mice were born in the ratio expected from Mendelian inheritance (Figure 1C and F) and were viable and fertile without any evident histopathological abnormalities. By using real-time quantitative PCR analysis, we have shown that the retinas of *HLF*$^{kd/kd}$ mice expressed HLF mRNA at about one-fifth that of wild type (Figure 1E). To investigate whether the reduced expression of HLF is due to insertion of the *neo* gene containing the double poly(A) signal, we deleted the *neo* gene cassette by mating *HLF*$^{kd/kd}$ mice with AYU-1-

Cre mice that ubiquitously express the Cre protein (Niwa *et al.*, 1993). Genotyping of the resulting offspring revealed that Cre recombinase successfully deleted the *neo* gene from the *HLF*^{kd} gene, leaving one remnant loxP in the first exon (*HLF*^{lox}) (Figure 1D). RT–PCR revealed that *HLF*$^{lox/lox}$ mice recovered a normal level of HLF mRNA expression comparable to that of the wild-type mice (Figure 1E).

Expression of HLF in mice homozygous for the HLF^{kd} gene

In *HLF*$^{kd/kd}$ mice, the expression of HLF mRNA was examined in various organs using real-time quantitative PCR (Figure 2A) and was reduced to 20–80%, depending on the organs, of wild type. The reason for this tissue-dependent variability in the reduced expression of HLF mRNA remains unknown. In contrast, the expression of HIF-1α mRNA in *HLF*$^{kd/kd}$ mice and wild-type mice did not differ in these organs (Figure 2B).

Hemorrhaging was not observed during the embryonic stages in *HLF*$^{kd/kd}$ mice (data not shown), and heart rate did not differ significantly between *HLF*$^{kd/kd}$ and wild-type mice at E18.5 (*HLF*$^{kd/kd}$: 28.3 ± 2.8, $n = 3$; wild type: 32.2 ± 6.6, $n = 5$).

Immunohistochemistry revealed that endothelial cells of the dorsal aorta and sympathetic cells at E10.5 (Figure 2C and F), adrenal gland at E15.5 (Figure 2D and G) and smooth muscle cells (Figure 2E and H) were stained positively with anti-HLF antibody in *HLF*$^{kd/kd}$ mice to a similar extent as in wild-type mice under the normoxic conditions.

Expression pattern of HLF in the mouse model of ROP

Immediately after hyperoxic treatment [postnatal day 12 (P12)–0 h] in the ROP model (Smith *et al.*, 1994) (Figure 3A), eyeballs were removed from the wild-type and *HLF*$^{kd/kd}$ mice. First, expression of HLF and HIF-1α was examined by western blotting of the eyes of wild-type and *HLF*$^{kd/kd}$ mice at different time points after a shift from hyperoxic to normoxic conditions. Induction of HLF was detected even at 2 h after the normoxia in wild-type mice, while essentially no induction of HLF was observed in *HLF*$^{kd/kd}$ mice during 12 h of normoxia (Figure 3C). Unexpectedly, HIF-1α expression displayed only a slight variation under hypoxic and normoxic conditions in wild-type mice, or in *HLF*$^{kd/kd}$ mice (Figure 3C).

Secondly, immunohistochemistry was performed to examine HLF and HIF-1α expression in the retinas of wild-type and *HLF*$^{kd/kd}$ mice. The normoxic treatment following the hypoxic conditions moderately enhanced the expression of HIF-1α in the inner nuclear layer (INL) and ganglion cell layer (GCL) of both the wild-type and the mutant mice (Figure 3H–K). On the other hand, the expression of HLF was induced in the wild type immediately after shift to normoxia (Figure 3D and E) whereas it was not induced in *HLF*$^{kd/kd}$ mice under subsequent normoxic conditions (Figure 3F and G). Although HLF and HIF-1α share many biochemical and transcriptional properties (Ema *et al.*, 1997; Wenger and Gassmann, 1997), their expression levels were independently regulated. The *HLF*$^{lox/lox}$ mice recovered enhanced HLF
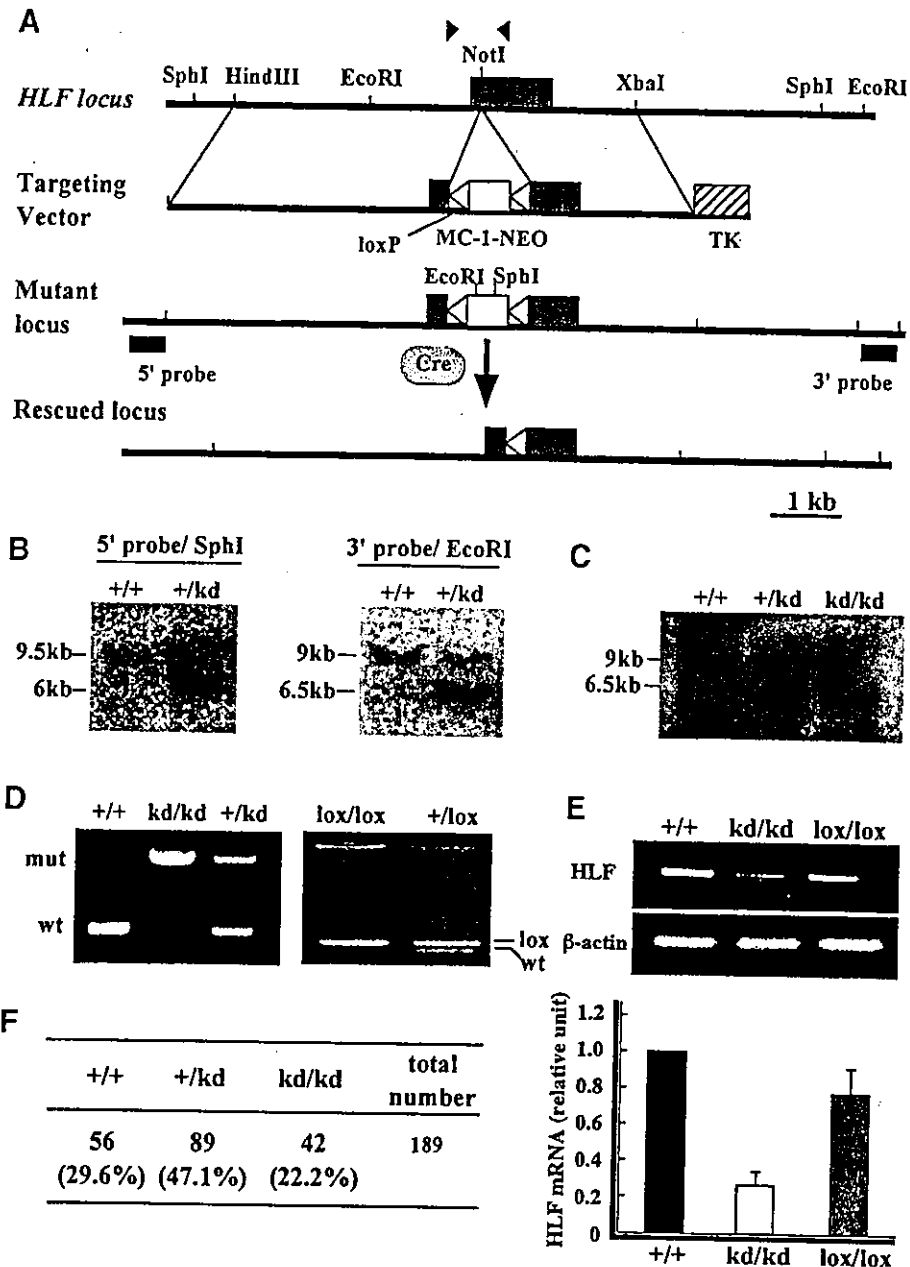
1135

Fig. 1. Mutation of mouse *HLF* gene. Outline of targeting vector and restriction maps around the first exon (closed box) (A). Arrowheads indicate the sites of primers used to distinguish the wild-type *HLF* gene from the mutant. MC-1-NEO (open box) indicates the neomycin resistance (*NEO*) gene under the control of the MC-1 promoter and TK is the thymidine kinase gene under the control of the herpes simplex virus promoter. The *NEO* gene sandwiched between loxP sequences was inserted into exon 1 at the *NotI* site. DNA blot analysis of DNAs from recombinant ES cells (B) or mouse tails (C). Genomic DNAs were digested with *SphI* or *Eco*RI, and hybridized with the 5' or 3' external probe, respectively. Genotyping of the *HLF* locus from offspring (D). PCR analyses were carried out with genomic DNAs from offspring generated by mating heterozygous *HLF*^{kd} mice (left panel). PCR analysis of the rescued *HLF*^{lox} gene is also shown (right panel). The inserted *NEO* gene was removed by mating *HLF*^{kd} mice with Cre-transgenic mice. RT–PCR analyses of HLF mRNA expression (E). RNAs were prepared from the eyes of wild-type, *HLF*$^{kd/kd}$ and *HLF*$^{lox/lox}$ mice, and subjected to RT–PCR analyses. Real-time quantitative PCR (bottom) was performed, and the amount of HLF mRNA from eyeballs of wild-type mice was designated as 1.0. Genotyping of littermates from the intercrosses of *HLF*$^{kd/+}$ heterozygotes 2 weeks after birth (F).

expression under relative hypoxic conditions, as observed in the wild type (data not shown).

Suppression of retinal neovascularization of *HLF*$^{kd/kd}$ mice

Under hyperoxic conditions in the ROP model, retinal capillary obliteration is observed (Smith *et al.*, 1994), and when mice are returned to room air (P12), they are considered to be exposed to relatively hypoxic conditions.

Subsequently, retinal neovascularization occurs in 100% of animals under these conditions with the increase in VEGF mRNA (Pierce *et al.*, 1995). In this ROP model, neovascularization in retinas was also reported to be maximal after 5 days of hyperoxic treatment followed by 5 days of relative hypoxia (P17) (Smith *et al.*, 1994). For reference, when kept under normal conditions, wild-type and *HLF*$^{kd/kd}$ mice showed essentially no difference in their retinal structures at P12 (Figure 4A and B) and
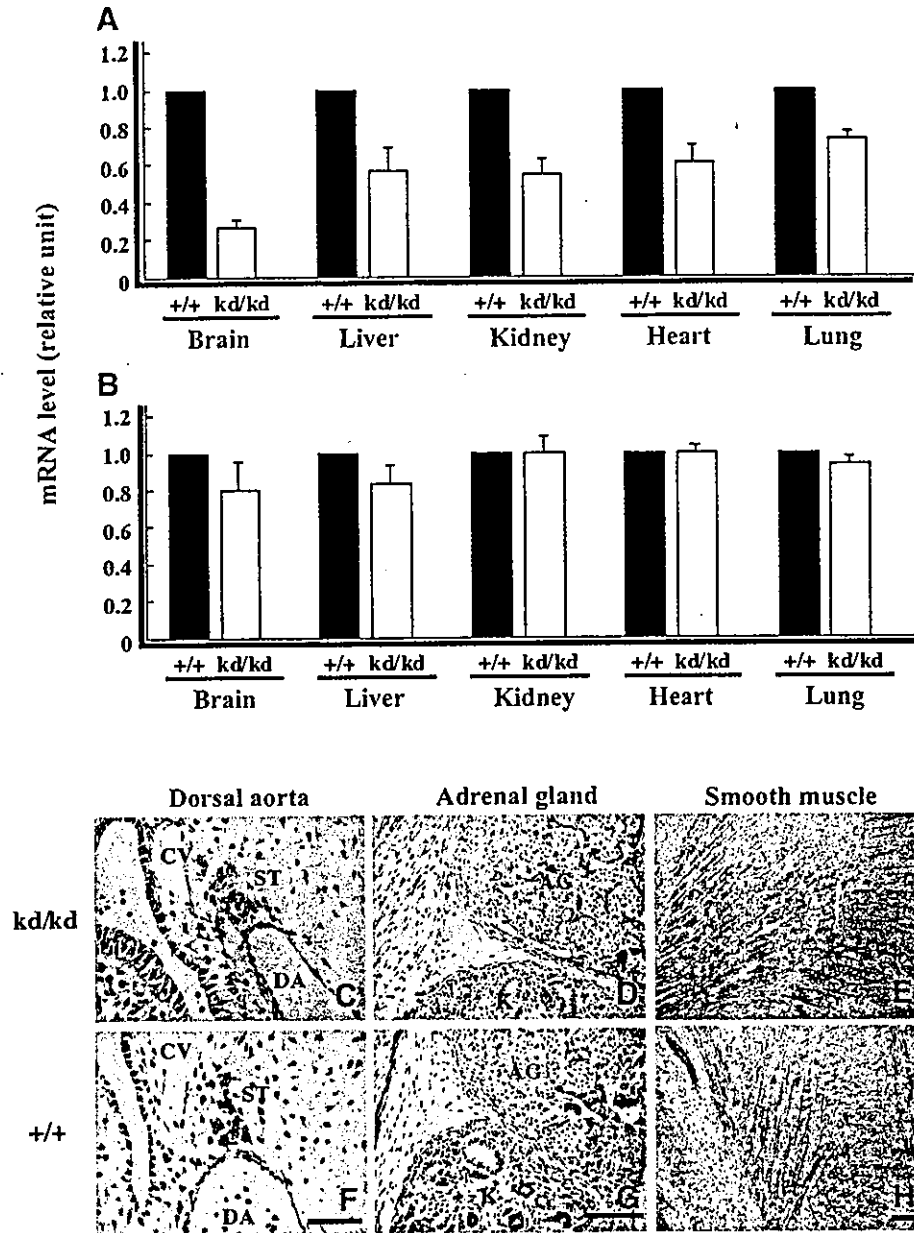
1136

Fig. 2. Comparison of HLF expression between wild-type and $HLF^{kd/kd}$ mice. Expression levels of HLF (A) and HIF-1α (B) mRNA were examined under normoxic conditions in various organs (brain, liver, kidney, heart and lung) by real-time quantitative PCR. Immunohistochemistry was undertaken by staining with anti-HLF antibody in the dorsal aorta, adrenal gland and smooth muscle of $HLF^{kd/kd}$ (C-E) and wild-type (F-H) mice at E18.5. Note that HLF was similarly expressed in $HLF^{kd/kd}$ and wild-type mice in each organ. Bars indicate 25 μm (F) and 100 μm (G and H). DA, dorsal aorta; CV, cardinal vein; ST, sympathetic trunk; AG, adrenal gland; K, kidney.

thereafter (data not shown). However, when wild-type mice were treated in the ROP model, multiple neovascularizations were induced at P17 on the vitreous side of the inner limiting membrane, with prominent neovascular tufts extending into the vitreous body (Figure 4D). In sharp contrast, there was essentially no neovascularization in the $HLF^{kd/kd}$ mice (Figure 4E). In total, 250 retinal cross-sections from each experimental group (three animals per group) were counted for neovascular buds to assess the extent of neovascularization, and the number was averaged per cross-section (Figure 4K). It was confirmed that neovascularization was remarkably induced in extent as well as in number in wild-type retinas by relative hypoxic

treatment. Strikingly, in $HLF^{kd/kd}$ mice, retinal neovascularization was almost completely suppressed on the inner retinal surface (Figure 4E and K).

To investigate whether the suppressed neovascularization is due to a lowered expression of HLF, the $HLF^{lox/lox}$ mice were subjected to the model of ROP. Interestingly, susceptibility to massive proliferative neovascularization, as found in wild-type mice, was recovered in the treated $HLF^{lox/lox}$ mice (Figure 4F and K). These results clearly demonstrated that the level of HLF expression is critical for ROP, and that the effects of the reduced expression of HLF cannot be compensated by HIF-1α. In the ROP model, neovascularization was investigated by staining

1137